

Frequency Domain Resampling for Gridded Spatial Data

SOUVICK BERA^{1,a}, DANIEL J. NORDMAN^{2,c} and SOUTIR BANDYOPADHYAY^{1,b}

¹*Department of Applied Mathematics and Statistics, Colorado School of Mines, Golden, CO 80401, USA,*

^aberasouvik@mines.edu, ^bsbandyopadhyay@mines.edu

²*Department of Statistics, Iowa State University, Ames, IA 50011, USA,* ^cdnordman@iastate.edu

In frequency domain analysis for spatial data, spectral averages based on the periodogram often play an important role in understanding spatial covariance structure, but also have complicated sampling distributions due to complex variances from aggregated periodograms. In order to nonparametrically approximate these sampling distributions for purposes of inference, resampling can be useful, but previous developments in spatial bootstrap have faced challenges in the scope of their validity, specifically due to issues in capturing the complex variances of spatial spectral averages. As a consequence, existing frequency domain bootstraps for spatial data are highly restricted in application to only special processes (e.g. Gaussian) or certain spatial statistics. To address this limitation and to approximate a wide range of spatial spectral averages, we propose a practical hybrid-resampling approach that combines two different resampling techniques in the forms of spatial subsampling and spatial bootstrap. Subsampling helps to capture the variance of spectral averages while bootstrap captures the distributional shape. The hybrid resampling procedure can then accurately quantify uncertainty in spectral inference under mild spatial assumptions. Moreover, compared to the more studied time series setting, this work fills a gap in the theory of subsampling/bootstrap for spatial data regarding spectral average statistics.

Keywords: Spatial Frequency Domain Bootstrap; Periodogram; Spectral Mean

1. Introduction

In recent years, there has been a marked increase in research on the analysis of spatial data using the frequency domain approach (see, for example, (Bandyopadhyay, Jentsch and Rao, 2017, Bandyopadhyay and Lahiri, 2010, Bandyopadhyay, Lahiri and Nordman, 2015, Bandyopadhyay and Rao, 2016, Fuentes, 2006, 2007, Hall, Fisher and Hoffman, 1994, Im, Stein and Zhu, 2007, Matsuda and Yajima, 2009, Van Hala et al., 2017, 2020)). As a benefit, analysis in the frequency domain allows inference about covariance structures through a data transformation (i.e., a Fourier or periodogram-based transform), without the need for a full probability model for spatial data. Resampling methods, such as subsampling and bootstrap, for spatial data have gained popularity in recent decades because these approaches can often allow for uncertainty quantification and distributional approximations for complicated spatial statistics in a nonparametric or model-free fashion; see (Davison and Hinkley, 1997, Sherman and Carlstein, 1994, Sherman, 1998). In a recent study, (Ng, Yau and Chen, 2021) introduced a type of frequency domain bootstrap (FDB) for Gaussian spatial data on grid. Although this work offers a significant contribution to nonparametric spatial approximations, the resampling methodology comes with certain hard limitations in application. Firstly, the FDB of (Ng, Yau and Chen, 2021) is generally not valid for approximating many spatial spectral averages of interest, because the latter have complex variance structures that this FDB proposal cannot correctly estimate. In particular, the challenge is that spectral mean statistics have variances that depend both on spatial covariances as well as higher order (i.e., fourth) process cumulants, which arise due to covariances between the spatial periodogram ordinates. Technically, it is the variance contributions related to higher order cumulants that are generally missed or ignored in the FDB approach of (Ng, Yau and Chen, 2021), unless the spatial data are

Gaussian (i.e., so that these variance components become zero). Consequently and secondly, the spatial bootstrap results of (Ng, Yau and Chen, 2021) are established under assumptions of Gaussianity, which can be stringent and may not suitably reflect the distributional nature of spectral average statistics in general practice. These aspects motivate a need to modify the spatial FDB of (Ng, Yau and Chen, 2021) to handle a broader range of spectral statistics with application potentially *non-Gaussian* spatial processes.

To provide improved and more universally valid distributional approximations with spatial spectral statistics, we introduce a resampling technique called spatial *Hybrid Frequency Domain Bootstrap* (HFDB) which aims to merge two different resampling schemes in the forms of subsampling and bootstrap into one overall approach in the frequency domain. The idea that spatial subsampling can be used to correctly estimate the variances of complicated spectral averages, while bootstrap can be used to re-create the shape of the sampling distributions. Essentially then, subsampling plays a role in appropriately modifying the spreads of FDB distributional approximations, where this bootstrap would otherwise be invalid without such scaling adjustments. The advantage of the proposed HFDB method is that this can accurately capture the uncertainty in spatial spectral statistics for calibrating tests or confidence intervals without requiring stringent conditions on the spatial processes or assumptions of Gaussianity; in particular, the conditions needed to validate HFDB basically amount to mild assumptions for ensuring that spectral averages have limit distributions at all. This work then intends to close some gaps in the scope of applying resampling approximations for spatial data, which is practically valuable. Additionally, our work also bridges some gaps in the theory of subsampling and bootstrap for spatial data, and extends some recent theoretical findings for spectral inference with time series to the spatial data setting.

We conclude this section by briefly overviewing FDB for time series and providing connections to the spatial bootstrap here. In time series analysis, FDB has received much attention and interest toward approximating the distributions of spectral statistics derived from the periodogram (cf. (Kreiss and Paparoditis, 2012, Kreiss and Lahiri, 2012, Lahiri, 2003, Politis and McElroy, 2019)). The key concept behind this method is to mimic a type of asymptotic independence that exists in the periodogram in order to generate versions of periodogram ordinates in the bootstrap world by independent resampling (cf. (Dahlhaus and Janas, 1996, Jentsch and Kreiss, 2010, Kreiss and Paparoditis, 2003, 2012, 2023, Kreiss, Paparoditis and Politis, 2011)). In the last three decades, there has been a progression of FDB methods, often relying on specific assumptions about the underlying time series (e.g., linear process) or differing cases of spectral mean parameters. Recently, a major advancement was achieved by (Meyer, Paparoditis and Kreiss, 2020) who introduced an innovative bootstrap method, called the hybrid periodogram bootstrap (HPB), that represents the state-of-the-art approach for time series inference concerning spectral means. Related to this, (Yu, Kaiser and Nordman, 2023) recently studied subsampling for use in conjunction with HPB, where subsampling helps to justify the latter bootstrap approach under weaker assumptions than (Meyer, Paparoditis and Kreiss, 2020) and so HPB extends to a wide range of application with various time processes. Unlike bootstraps that aim to re-create statistics at the same data level as the original sample, subsampling is a different resampling approach that generates smaller-scale copies of statistic; because of this distinction, subsampling often applies under weaker conditions than bootstrap, though bootstrap can provide more accurate distributional approximations when valid (cf. (Politis, Romano and Wolf, 1999)). The spatial FDB proposed by (Ng, Yau and Chen, 2021) is the spatial equivalent of one of the original FDB methods for time series (cf. (Dahlhaus and Janas, 1996, Jentsch and Kreiss, 2010, Kreiss and Paparoditis, 2003)), while the proposed spatial HFDB here intends to be a spatial analog of the HPB for time series as studied in (Meyer, Paparoditis and Kreiss, 2020) when combined with a subsampling extension as in (Yu, Kaiser and Nordman, 2023). This development is non-trivial for spatial data and, similar to the time series setting, is crucial for avoiding restrictive process and moment conditions for dependent data. Finally, it is worth mentioning that, similar to (Ng, Yau and Chen, 2021), we focus our resampling presentation on spatial

observations lying on a lattice in two-dimensional space, though findings can be extended to gridded data in more general spatial sampling dimensions $d \geq 2$.

The remainder of the paper is organized as follows. Section 2 introduces the distributions of spectral mean statistics, which form the basis for inference, along with the associated framework. Section 3 presents a spatial subsampling framework in the frequency domain and establishes its consistency, forming the foundation for the proposed bootstrap procedure. A detailed discussion of the hybrid bootstrap method for spatial data is provided in Section 4. Section 5 presents numerical studies to evaluate the accuracy of the proposed procedure, and Section 6 demonstrates an application for calibrating spatial isotropy tests. Finally, Section 7 concludes with key insights. Additional technical details and simulation results can be found in [Appendix](#) and [Supplementary Material](#), respectively.

2. Distributions of Spectral Mean Statistics

2.1. Spatial process and sampling design

Throughout this paper, we follow spatial sampling framework similar to ([Bandyopadhyay and Lahiri, 2010](#)) and ([Ng, Yau and Chen, 2021](#)). Let $\{Z(\mathbf{s}) : \mathbf{s} \in \mathbb{Z}^2\}$ denote a real-valued second-order stationary process located on a regular integer grid \mathbb{Z}^2 . In this fashion, potential observations lie on a spatial lattice with a constant separation in each coordinate direction (which we take to be 1 though other scaling is possible as well). We assume that the random process $Z(\mathbf{s})$ is observed at $n \equiv n_1 n_2$ sampling sites defined by

$$\{\mathbf{s}_1, \dots, \mathbf{s}_n\} = \{\mathbf{s} \in \mathbb{Z}^2 : \mathbf{s} \in \mathcal{D}(n_1 \times n_2)\} = \mathcal{D}(n_1 \times n_2) \cap \mathbb{Z}^2$$

given by those locations on the grid \mathbb{Z}^2 that lie within a rectangular sampling region $\mathcal{D}(n_1 \times n_2) \equiv [1, n_1] \times [1, n_2]$ for integers $n_1, n_2 \geq 1$.

For spatial data analysis, the above sampling framework corresponds to a so-called pure increasing domain for developing spatial results (cf. ([Cressie, 1993](#))). That is, in this scheme, more spatial observations are available (i.e., $n \rightarrow \infty$) as spatial sampling region expands in size in each direction (i.e., $n_i \rightarrow \infty$ for $i = 1, 2$).

2.2. Spectral mean parameters

Suppose that the second order stationary spatial process $\{Z(\mathbf{s}) : \mathbf{s} \in \mathbb{Z}^2\}$ has a spectral density denoted as $f(\boldsymbol{\omega}) : \Pi^2 \rightarrow [0, \infty)$ where $f(\boldsymbol{\omega}) \equiv (2\pi)^{-2} \sum_{\mathbf{h} \in \mathbb{Z}^2} \text{Cov}(Z(\mathbf{0}), Z(\mathbf{h})) \exp(-i\mathbf{h}^\top \boldsymbol{\omega})$, for $\boldsymbol{\omega} \equiv \sqrt{-1}$ and for $\boldsymbol{\omega} \in \Pi^2 \equiv [-\pi, \pi]^2$. Then, the target spatial parameter for inference is a *spectral mean* parameter defined as an integral

$$M(\psi) = \int_{\Pi^2} \psi(\boldsymbol{\omega}) f(\boldsymbol{\omega}) d\boldsymbol{\omega}, \quad (1)$$

involving f and some chosen/given function $\psi : \Pi^2 \rightarrow \mathbb{R}$ of bounded variation. Spectral mean parameters are common in the spatial data analysis for studying the spatial covariance structure of the data with an unknown distribution. Such quantities have a well-established history for both time series and spatial data (see, ([Politis and McElroy, 2019](#)) for more details), dating as far back as ([Parzen, 1957](#)), and many spatial parameters of interest can be expressed in the form of a spectral mean. Standard examples of spectral means include autocovariances and spectral distributions, as described below, depending on the choice of ψ above. Next we give some examples of spectral mean parameters arising in frequency

domain analysis (cf. (Bandyopadhyay, Lahiri and Nordman, 2015, Dahlhaus, 1985, Dahlhaus and Janas, 1996, Parzen, 1957, Subba Rao, 2018, Van Hala et al., 2017, 2020) and the references therein).

Examples of spectral mean parameters

1. *Covariance function.* For a lag vector $\mathbf{h} \in \mathbb{Z}^2$, if we consider the function $\psi(\omega) = \cos(\mathbf{h}^T \omega)$ in 1, this leads to the autocovariance function $\gamma(\mathbf{h}) = \text{Cov}(Z(\mathbf{0}), Z(\mathbf{h}))$, which can be viewed as a spectral mean $M(\psi)$. Note that, for testing the special hypothesis $H_0 : Z(\mathbf{s})$ is white noise (constant f), a test based on the process autovariances can be applied, similar to some Portmanteau tests (cf. (Li and McLeod, 1986, Ljung and Box, 1978)) using the fact that the spectral means $M(\psi)$ are zero under this H_0 for the function choice $\psi(\omega) \equiv [\cos(\mathbf{h}_1^T \omega), \dots, (\cos(\mathbf{h}_k^T \omega))]^T$ for some integer lags $\mathbf{h}_1, \dots, \mathbf{h}_k$.

2. *Spectral distribution function.* For a vector $\mathbf{t} \in \mathbb{R}^2$, the spectral distribution function is defined as $F(\mathbf{t}) = \int_{\mathbb{R}^2} \mathbb{I}_{(-\infty, \mathbf{t}]}(\omega) f(\omega) d\omega$, which corresponds to a spectral mean parameter defined by $\gamma(\mathbf{h}) = \mathbb{I}_{(-\infty, \mathbf{t}]}(\omega)$ in (1) where $\mathbb{I}(\cdot)$ is the indicator function and $(-\infty, \mathbf{t}] \equiv (-\infty, t_1] \times (-\infty, t_2]$. The spectral distribution function plays an important role in determining the smoothness of the sample paths of the spatial process $Z(\cdot)$ (cf. (Stein, 1999)).

3. *Assessment of spatial covariance structures.* When analyzing spatial data, it can be useful to assess the spatial covariance structures in a nonparametric manner, without requiring specific distributional assumptions about the data. General testing methods can be developed of evaluating different hypotheses about spatial covariances, such as tests of isotropy or separability, by examining $M(\psi)$ with appropriate choices of $\psi(\omega)$ functions. For more details, refer to (Van Hala et al., 2017, 2020).

4. *Whittle Estimation.* Suppose $\{f_\theta\}$ represents a parametric family of spectral densities (indexed by θ). Whittle estimation aims to identify the closest member f_θ to the true density f (cf. (Taniguchi, 1979)). Assuming real-valued θ for illustration, the solution to a spectral mean equation $M(\psi) = 0$ identifies the appropriate f_θ under certain conditions, using a function $\psi(\omega) \equiv [1 - f_\theta(\omega)/f(\omega)] \frac{d}{d\theta} f_\theta^{-1}(\omega)$, $\omega \in \mathbb{R}^2$, defined by the derivative of $f_\theta^{-1}(\omega) \equiv 1/f_\theta(\omega)$.

5. *Goodness-of-fit tests.* There has been increasing interest in frequency domain based tests to assess model adequacy (cf. (Crujeiras and Fernandez-Casal, 2010, Van Hala et al., 2020, Weller and Hoeting, 2020)). Consider a test involving a simple null hypothesis $H_0 : f = f_0$ against an alternative $H_0 : f \neq f_0$ for some candidate spectral density f_0 . One immediate test for H_0 is based on the function $\psi(\omega) = 1/f_0(\omega)$ with $M(\psi)$ a constant under this simple H_0 . To test the composite hypothesis $H_0 : f \in \mathcal{F}$ for a specified parametric class \mathcal{F} , several frequency domain tests have been proposed in time series (cf. (Beran, 1992), (Milhøj, 1981), (Paparoditis, 2000), (Nordman and Lahiri, 2006)). These tests can use Whittle estimation to choose the “best” fitting model from \mathcal{F} and then compare the fitted density to the periodogram across all ordinates. One can adapt strategies for goodness-of-fit tests with time series (cf. (Nordman and Lahiri, 2006)), which combine aspects of model fitting and model comparison into a choice of estimating function ψ , to spatial processes.

6. *Variogram model fitting.* A popular approach to fitting a parametric variogram model to spatial data is through the method of least squares; see (Cressie, 1993). Let $\{2\gamma(\cdot; \theta) : \theta \in \Theta\}$, $\Theta \subset \mathbb{R}^p$ denote a class of valid variogram models for the true variogram $2\gamma(\mathbf{h}) \equiv \text{Var}(Z(\mathbf{h}) - Z(\mathbf{0}))$, $\mathbf{h} \in \mathbb{Z}^2$ of the spatial process. Let $2\hat{\gamma}_n(\mathbf{h})$ denote the sample variogram at lag \mathbf{h} based on $Z(\mathbf{s}_1), \dots, Z(\mathbf{s}_n)$ (cf. Chapter 2, (Cressie, 1993)). Then one can fit the variogram model by estimating the parameter θ that minimizes the criterion: $\hat{\theta}_n = \text{argmin} \left\{ \sum_{i=1}^m \left(2\hat{\gamma}_n(\mathbf{h}_i) - 2\gamma(\mathbf{h}_i; \theta) \right)^2 : \theta \in \Theta \right\}$ for a given set of lags $\mathbf{h}_1, \dots, \mathbf{h}_m$. Expressing the variogram in terms of the spectral density function, we get an equivalent spectral esti-

inating equation for identifying θ : $M(\psi) = 0$ for

$$M(\psi) \equiv \int_{\mathbb{R}^2} \left[\sum_{i=1}^m \left\{ 1 - \cos(\mathbf{h}_i^T \omega) - \gamma(\mathbf{h}; \theta) \right\} \nabla[2\gamma(\mathbf{h}_i; \theta)] \right] f(\omega) d\omega,$$

using $\psi_\theta(\omega) \equiv \sum_{i=1}^m \left\{ 1 - \cos(\mathbf{h}_i^T \omega) - \gamma(\mathbf{h}; \theta) \right\} \nabla[2\gamma(\mathbf{h}_i; \theta)]$.

2.3. Spectral mean statistics and sampling distributions

Based on the stationary spatial process $Z(\cdot)$ as observed on the sampling region $\mathcal{D}(n_1 \times n_2)$, where $n = n_1 n_2$ is the number of observations, we define $\mathcal{I}_n(\omega)$ to be the periodogram at a frequency $\omega \in \Pi^2$ as

$$\mathcal{I}_n(\omega) \equiv (2\pi)^{-2} n^{-1} \left| \sum_{s_1=1}^{n_1} \sum_{s_2=1}^{n_2} Z(\mathbf{s}) \exp(-i\mathbf{s}^T \omega) \right|^2, \quad \mathbf{s} \equiv (s_1, s_2)^T, \quad \text{where } i = \sqrt{-1}.$$

Using $\mathcal{I}_n(\cdot)$ in place of $f(\cdot)$ in (1), a standard estimator of the spectral mean parameter $M(\psi)$ is then the *spectral mean statistic*, or *spectral average*, given in Riemann sum form by

$$\hat{M}_n(\psi) \equiv (2\pi)^2 n^{-1} \sum_{\mathbf{j} \in \mathcal{J}_n} \psi(\omega_{\mathbf{j},n}) \mathcal{I}_n(\omega_{\mathbf{j},n}),$$

using discrete frequencies $\omega_{\mathbf{j},n} \equiv (2\pi j_1/n_1, 2\pi j_2/n_2)$ defined by $\mathbf{j} \equiv (j_1, j_2) \in \mathcal{J}_n$ with index set $\mathcal{J}_n \equiv \{ \lfloor -(n_1 - 1)/2 \rfloor, \dots, n_1 - \lfloor n_1/2 \rfloor \} \times \{ \lfloor -(n_2 - 1)/2 \rfloor, \dots, n_2 - \lfloor n_2/2 \rfloor \} \setminus \{(0, 0)\}$ denoting the (nonzero) discrete Fourier frequency grid. For calibrating tests and confidence intervals, a spectral mean statistic has a large-sample normal distribution under mild conditions (Brillinger, 2001, Dahlhaus, 1985) given by

$$H_n(\psi) \equiv n^{1/2} \{ \hat{M}_n(\psi) - M(\psi) \} \xrightarrow{D} \mathcal{N}(0, \sigma^2 = \sigma_1^2 + \sigma_2^2) \text{ as } n \rightarrow \infty, \quad (2)$$

with

$$\begin{aligned} \sigma_1^2 &\equiv \sigma_1^2(\psi) = (2\pi)^2 \int_{\Pi^2} \psi(\omega) [\psi(\omega) + \psi(-\omega)] f^2(\omega) d\omega, \\ \sigma_2^2 &\equiv \sigma_2^2(\psi) = (2\pi)^2 \int_{\Pi^2} \int_{\Pi^2} \psi(\omega_1) \psi(\omega_2) f_4(\omega_1, \omega_2, -\omega_2) d\omega_1 d\omega_2 \end{aligned}$$

where, for $\omega_1, \omega_2, \omega_3 \in \Pi^2$,

$$f_4(\omega_1, \omega_2, \omega_3) = (2\pi)^{-3} \sum_{\mathbf{h}_1, \mathbf{h}_2, \mathbf{h}_3 \in \mathbb{Z}^2} \text{cum}(Z(\mathbf{0}), Z(\mathbf{h}_1), Z(\mathbf{h}_2), Z(\mathbf{h}_3)) \exp\left(-i \sum_{\ell=1}^3 \mathbf{h}_\ell^T \omega_\ell\right),$$

denotes the 4th-order cumulant spectral density. Given the complicated structure in the limit distribution from (2), one possible approach is to explore resampling for approximating the distribution of $H_n(\psi)$ nonparametrically. However, estimation of the variance component σ_2^2 , in particular, poses significant challenges for bootstrap approximations to the distribution of $H_n(\psi)$, as needed for the inference of spatial mean parameters. Specially, the spatial FDB introduced in (Ng, Yau and Chen, 2021)

cannot capture this component in general, unless the underlying process is assumed to be Gaussian in which case this variance component $\sigma_2^2 = 0$ becomes zero. As a consequence, in order to improve bootstrap inference for spatial data, one must first correctly estimate all variance components in (2) in the resampling mechanism used. For use in conjunction with spatial bootstrap, we next consider a spatial subsampling for the purpose of such variance estimation, as described in the following section.

3. Spatial Subsampling in Frequency Domain

3.1. Spatial subsampling variance estimators

Based on the observed spatial data $\{Z(\mathbf{s}) : \mathbf{s} \in \mathcal{D}(n_1 \times n_2) \cap \mathbb{Z}^2\}$ lying within the spatial sampling region $\mathcal{D}(n_1 \times n_2) \equiv [1, n_1] \times [1, n_2]$, subsampling aims to create several “smaller scale copies” of the original spatial data by using data blocks of smaller size $b_n \equiv n_1^{(b)} n_2^{(b)}$ with $n_k^{(b)} < n_k$, $k = 1, 2$ (cf. (Lahiri, 2003, Sherman and Carlstein, 1994, Sherman, 1996, 1998)) compared to $n = n_1 n_2$, where the block size $n_k^{(b)}$ and the original sample size n_k in each direction satisfy the relation $n_k^{(b)} \rightarrow \infty$ and $n_k^{-1} n_k^{(b)} \rightarrow 0$ as $n \rightarrow \infty$. In particular, we can define data blocks by all integer translates of a region $\mathcal{D}(n_1^{(b)} \times n_2^{(b)}) \equiv [1, n_1^{(b)}] \times [1, n_2^{(b)}]$ that lie inside the original sampling region $\mathcal{D}(n_1 \times n_2) \equiv [1, n_1] \times [1, n_2]$; that is, each data block is of the form $\mathbf{j} + \mathcal{D}(n_1^{(b)} \times n_2^{(b)})$ for an integer $\mathbf{j} \equiv (j_1, j_2)$ with components $j_k = 0, \dots, n_k - n_k^{(b)}$, $k = 1, 2$. In total, there are, say $L \equiv (n_1 - n_1^{(b)} + 1)(n_2 - n_2^{(b)} + 1)$, such data blocks and, for simplicity, we can denote the ℓ -data block as \mathcal{B}_ℓ for $\ell = 1, \dots, L$. We can then define a subsample periodogram for the ℓ -th block as

$$I_{sub}^{(\ell)}(\omega) \equiv (2\pi)^{-2} b_n^{-1} \left| \sum_{\mathbf{s} \in \mathcal{B}_\ell \cap \mathbb{Z}^2} Z(\mathbf{s}) e^{-i\mathbf{s}^T \omega} \right|^2, \quad \omega \in \Pi^2, \ell = 1, \dots, L.$$

The corresponding subsample analogue of the mean statistic $\widehat{M}_n(\psi)$ can then be defined as

$$\widehat{M}_{sub}^{(\ell)}(\psi) \equiv (2\pi)^2 b_n^{-1} \sum_{\mathbf{j} \in \mathcal{J}_b} \psi(\omega_{\mathbf{j},b}) I_{sub}^{(\ell)}(\omega_{\mathbf{j},b}),$$

where $\omega_{\mathbf{j},b}$ and \mathcal{J}_b are defined in a manner similar to $\omega_{\mathbf{j},n}$ and \mathcal{J}_n earlier, but now based on the subsample sizes b_n rather than the original data size n . These lead to a collection of subsample versions $H_{sub}^{(\ell)}(\psi)$ of the target spectral quantity $H_n(\psi) \equiv n^{1/2} \{\widehat{M}_n(\psi) - M(\psi)\}$ as

$$H_{sub}^{(\ell)}(\psi) \equiv b_n^{1/2} \{\widehat{M}_{sub}^{(\ell)}(\psi) - \widetilde{M}_n(\psi)\}, \quad \ell = 1, \dots, L,$$

using the subsample mean $\widetilde{M}_n(\psi) = L^{-1} \sum_{\ell=1}^L \widehat{M}_{sub}^{(\ell)}(\psi)$ which substitutes the unknown parameter $M(\psi)$.

Recall that spatial variance estimation is especially important here because the variance σ^2 of spectral mean statistics from (2) can be quite complex or difficult to determine accurately, which is our motivation for consideration of subsampling. Consequently, we can define the subsampling variance estimator of σ^2 as

$$\widehat{\sigma}_n^2 = \widehat{\sigma}_n^2(\psi) \equiv \int_{\mathbb{R}} z^2 d\widehat{F}_{H_n(\psi)}(z) = L^{-1} \sum_{\ell=1}^L b_n \{\widehat{M}_{sub}^{(\ell)}(\psi) - \widetilde{M}_n(\psi)\}^2, \quad (3)$$

which corresponds to the sample variance of the subsample statistics $\{H_{sub}^{(\ell)}(\psi) \equiv b_n^{1/2} \widehat{M}_{sub}^{(i)}(\psi)\}_{\ell=1}^L$. Further, using subsampling, we also introduce an estimator for just the first variance component $\sigma_1^2(\psi)$ in (2) as

$$\widehat{\sigma}_{1,n}^2 = b_n^{-1} (4\pi^2)^2 \sum_{\mathbf{j} \in \mathcal{J}_b} \psi(\omega_{\mathbf{j},b}) (\psi(\omega_{\mathbf{j},b}) + \psi(\omega_{-\mathbf{j},b})) \frac{1}{L} \sum_{\ell=1}^L (\mathcal{I}_{sub}^{(\ell)}(\omega_{\mathbf{j},b}) - \widetilde{\mathcal{I}}_n(\omega_{\mathbf{j},b}))^2, \quad (4)$$

where $\widetilde{\mathcal{I}}_n(\omega_{\mathbf{j},b}) \equiv L^{-1} \sum_{\ell=1}^L \mathcal{I}_{sub}^{(\ell)}(\omega_{\mathbf{j},b})$. Here in (4), we are isolating a component from the overall subsampling variance estimator σ_n^2 in (3) that arises due to marginal variances in subsample periodogram $\{\mathcal{I}_{sub}^{(\ell)}(\omega_{\mathbf{j},b})\}_{\ell=1}^L$. This leads to a second subsampling estimator

$$\widehat{\sigma}_{2,n}^2 \equiv \widehat{\sigma}_n^2 - \widehat{\sigma}_{1,n}^2 \quad (5)$$

to approximate the second or remaining component $\sigma_2^2(\psi)$ in (2). Spatial subsampling then enables a valid estimation of both variance components σ_1^2 and σ_2^2 which contribute to the target distribution of $H_n(\psi)$ having a limit variance of $\sigma^2 \equiv \sigma_1^2 + \sigma_2^2$.

3.2. Consistency of spatial subsampling estimators

To establish the formal consistency properties for subsampling variance estimators with respect to spectral mean statistics, we use the following mild assumptions, related to the existence of limit laws.

Assumption 1. $\{Z(\mathbf{s}) : \mathbf{s} \in \mathbb{Z}^2\}$ is 4-th order stationary.

Assumption 2. The limiting law in (2) exists for any ψ of bounded variation.

For two sequences $\mathbf{j}^{(n)} \equiv (j_1^{(n)}, j_2^{(n)})$, $\mathbf{k}^{(n)} \equiv (k_1^{(n)}, k_2^{(n)}) \in \mathbb{Z}^2$ of integer pairs, define $H_{\mathbf{j}^{(n)},n}(\psi)$ and $H_{\mathbf{k}^{(n)},n}(\psi)$ as versions of $H_n(\psi)$ when computed from translated spatial regions $\mathbf{j}^{(n)} + \mathcal{D}(n_1 \times n_2)$ and $\mathbf{k}^{(n)} + \mathcal{D}(n_1 \times n_2)$, instead of the region $\mathcal{D}(n_1 \times n_2) \equiv [1, n_1] \times [1, n_2]$ used for $H_n(\psi)$ in (2).

Assumption 3. For any two $\mathbf{j}^{(n)}$ and $\mathbf{k}^{(n)}$ integer sequences whereby $|j_i^{(n)} - k_i^{(n)}|/n_i \rightarrow \infty$ holds for $i = 1, 2$ as $n \equiv n_1 \times n_2 \rightarrow \infty$, then the following quantities are asymptotically normal and independent:

$$\begin{pmatrix} H_{\mathbf{j}^{(n)},n}(\psi) \\ H_{\mathbf{k}^{(n)},n}(\psi) \end{pmatrix} \xrightarrow{D} \mathcal{N} \left(\begin{pmatrix} 0 \\ 0 \end{pmatrix}, \sigma^2(\psi) \begin{pmatrix} 1 & 0 \\ 0 & 1 \end{pmatrix} \right) \quad \text{as } n \rightarrow \infty.$$

For two integer sequences $\mathbf{j}^{(n)}, \mathbf{k}^{(n)} \in \mathbb{Z}^2$, we use one further assumption stated below that relates to the periodogram, say $\mathcal{I}_{\mathbf{j}^{(n)},n}(\omega)$ and $\mathcal{I}_{\mathbf{k}^{(n)},n}(\omega)$, when computed on translated sampling regions $\mathbf{j}^{(n)} + \mathcal{D}(n_1 \times n_2)$ and $\mathbf{k}^{(n)} + \mathcal{D}(n_1 \times n_2)$, respectively, for $\omega \in \Pi^2 \equiv [-\pi, \pi]^2$.

Assumption 4. Let $\mathbf{m}_n \equiv (m_{n_1}, m_{n_2}) \in \mathbb{Z}^2$ with $0 \leq |m_{n_i}| \leq n_i - \lfloor n_i/2 \rfloor$, $i = 1, 2$ be an integer sequence such that the discrete Fourier frequencies $\omega_{\mathbf{m}_n,n}$ converge to some limit $\omega \equiv (\omega_1, \omega_2)$ with $0 < |\omega_i| < \pi$, $i = 1, 2$, as $n \equiv n_1 \times n_2 \rightarrow \infty$. For any two $\mathbf{j}^{(n)}$ and $\mathbf{k}^{(n)}$ integer sequences whereby $|j_i^{(n)} - k_i^{(n)}|/n_i \rightarrow \infty$

holds for $i = 1, 2$ as $n \equiv n_1 \times n_2 \rightarrow \infty$, then the following quantities are asymptotically exponential and independent:

$$\begin{pmatrix} \mathcal{I}_{\mathbf{j}^{(n)},n}(\omega_{\mathbf{m}_n,n}) \\ \mathcal{I}_{\mathbf{k}^{(n)},n}(\omega_{\mathbf{m}_n,n}) \end{pmatrix} \xrightarrow{D} f(\omega) \begin{pmatrix} U_1 \\ U_2 \end{pmatrix} \quad \text{as } n \rightarrow \infty$$

where U_1, U_2 denote i.i.d standard exponential random variables.

To comment on the conditions, Assumptions 1-2 together guarantee that $H_n(\psi)$ has a valid limiting law, while $\sigma^2(\psi)$ is finite by Assumption 1. Assumption 3 is a mild characterization of weak dependence in terms of the limit distributions of well-separated statistics and is also strongly connected to Assumptions 1-2. This condition states that any two copies $H_{\mathbf{j}^{(n)},n}(\psi)$ and $H_{\mathbf{k}^{(n)},n}(\psi)$ of the statistical quantity of interest $H_n(\psi)$, when defined on size $n \equiv n_1 \times n_2$ regions that are distantly separated, should be normal and asymptotically independent as $n \equiv n_1 \times n_2 \rightarrow \infty$; in particular, the spatial regions $\mathbf{j}^{(n)} + \mathcal{D}(n_1 \times n_2)$ and $\mathbf{k}^{(n)} + \mathcal{D}(n_1 \times n_2)$ for defining $H_{\mathbf{j}^{(n)},n}(\psi)$ and $H_{\mathbf{k}^{(n)},n}(\psi)$ are indeed distantly separated in the sense that i th component of the difference $\mathbf{j}^{(n)} - \mathbf{k}^{(n)}$ diverges faster than the sample size n_i in each direction, $i = 1, 2$. Assumption 4 is analogous to Assumption 3 in spirit but generally weaker. Assumption 4 says that spatial periodograms computed from distant regions should be asymptotically independent and have exponential distributions up to scaling by the spectral density f ; this is also a mild condition related to weak spatial dependence. Assumptions 1-4 are generally intended to hold for many spatial processes, without requiring more specific characterizations of spatial dependence in terms of linearity or forms of mixing (cf. (Lahiri, 2003, Yu, Kaiser and Nordman, 2023)).

We can next state a formal result on the consistency of subsampling variance estimators for spatial spectral mean statistics.

Theorem 3.1. Suppose Assumptions 1-4 hold and the subsample size $b_n \equiv n_1^{(b)} \times n_2^{(b)}$ satisfies $1/n_k^{(b)} + n_k^{-1}n_k^{(b)} \rightarrow 0$ for $k = 1, 2$ as $n \equiv n_1 \times n_2 \rightarrow \infty$. Then, the spatial subsampling estimators of variance components are consistent:

$$\widehat{\sigma}_{1,n}^2 \xrightarrow{P} \sigma_1^2, \quad \widehat{\sigma}_{2,n}^2 \xrightarrow{P} \sigma_2^2, \quad \text{and} \quad \widehat{\sigma}_n^2 \xrightarrow{P} \sigma^2 \equiv \sigma_1^2 + \sigma_2^2 \quad \text{as } n \rightarrow \infty.$$

The theorem above provides a device to modify and improve spatial bootstraps for approximating spectral mean statistics, particularly when such bootstraps can fail to appropriately reflect the spreads of such statistics. This then leads to the spatial hybrid bootstrap procedure proposed in the next section.

4. Spatial Hybrid Frequency Domain Bootstrap (HFDB)

We may now describe our main resampling approach for approximating the distribution of spatial spectral mean statistics. Recall that, as explained in the Introduction, (Ng, Yau and Chen, 2021) proposed a bootstrap for spatial data, which is generally invalid for inference about spectral averages and requires modification for capturing the complicated variance of spectral averages. For reference, we shall term their bootstrap method as technically being a Frequency Domain Wild Bootstrap (FDWB). Recently, for the case of time series data, (Meyer, Paparoditis and Kreiss, 2020) and (Yu, Kaiser and Nordman, 2023) described a hybrid periodogram bootstrap (HPB) as the most advanced resampling scheme for spectral mean inference with time series in terms of broad validity and performance. Our hybrid resampling approach for spatial data, termed the Hybrid Frequency Domain Bootstrap (HFDB), intends types of extensions of both FDWB and HPB methods. That is, the spatial HFDB aims to combine spatial bootstrap (i.e., FDWB) with spatial subsampling (Sec. 3.1) in order to correct scaling issues

in bootstrap for spatial data. This also produces a spatial analog version of HPB from time series, as explained more in the following.

For setting distributional approximations for spatial spectral mean statistics, both HFDB and FDWB approaches start with a common step of mimicking the distribution of spectral statistics by a scheme of independently resampling or re-creating periodogram values based on an estimator \hat{f}_n of the spectral density f . To this end, let \hat{f}_n represent a consistent estimator of the spectral density f across spatial discrete Fourier frequencies, i.e.

$$\max_{\mathbf{j} \in \mathcal{J}_n} |\hat{f}_n(\omega_{\mathbf{j},n}) - f(\omega_{\mathbf{j},n})| = o_P(1) \text{ as } n \rightarrow \infty. \quad (6)$$

Note that all FDB approaches involve spectral density estimation, which is true for time series (cf. (Dahlhaus and Janas, 1996, Jentsch and Kreiss, 2010, Kreiss and Paparoditis, 2003, Meyer, Paparoditis and Kreiss, 2020)) as well as for FDWB with spatial data as in (Ng, Yau and Chen, 2021). We then define an initial bootstrap re-creation of the target spectral mean quantity $H_n(\psi)$ from (2) as

$$Q_{FDWB,n}^*(\psi) \equiv n^{1/2} \{ (2\pi)^2 n^{-1} \sum_{\mathbf{j} \in \mathcal{J}_n} \psi(\omega_{\mathbf{j},n}) \hat{f}_n(\omega_{\mathbf{j},n}) (U_{\mathbf{j}}^* - 1) \} \quad (7)$$

by drawing $U_{\mathbf{j}}^*$ as i.i.d exponential random variables for indices $\mathbf{j} \equiv (j_1, j_2) \in \mathcal{J}_n$ involving $j_1 > 0$ or involving $j_1 = 0$ with $j_2 > 0$ and then setting $U_{-\mathbf{j}}^* \equiv U_{\mathbf{j}}^*$ for the remaining indices $\mathbf{j} \in \mathcal{J}_n$ (i.e., where $j_1 < 0$ or where $j_1 = 0$ with $j_2 < 0$). Note that the bootstrap approximation in (7) corresponds to the FDWB of (Ng, Yau and Chen, 2021) for spatial data and also represents a basic step in any FDB with time series (cf. (Meyer, Paparoditis and Kreiss, 2020)). This bootstrap form aims to produce bootstrap versions $\{U_{\mathbf{j}}^* \hat{f}_n(\omega_{\mathbf{j},n})\}$ of the periodogram ordinates $\{I_n(\omega_{\mathbf{j},n})\}$ (i.e., indexed over $\mathbf{j} \in \mathcal{J}_n$), by treating the latter as approximately independent exponential variables with respective means $\{f(\omega_{\mathbf{j},n})\}$. However, the problem in this bootstrap re-creation is that dependence among periodogram ordinates $I_n(\omega_{\mathbf{j},n})$, $\mathbf{j} \in \mathcal{J}_n$, is generally not completely ignorable so the bootstrap quantity $Q_{FDWB,n}^*(\psi)$ cannot correctly capture the true variance $\sigma^2 \equiv \sigma_1^2 + \sigma_2^2$ of $H_n(\psi)$ in (2). Essentially, by independently resampling or re-constructing spatial periodogram values by $\{U_{\mathbf{j}}^* \hat{f}_n(\omega_{\mathbf{j},n})\}$, the resulting FDWB in (7) then estimates the second variance component σ_2^2 to be zero, where the latter may not hold in general for the underlying spatial process (i.e., unless the process is assumed to be Gaussian).

To overcome the above shortcoming in FDWB, a scaling adjustment with spatial subsampling can be made to define a hybrid FDB (HFDB) rendition of $H_n(\psi)$ as

$$H_{HFDB,n}^*(\psi) \equiv [\text{Var}_* \{Q_{FDWB,n}^*(\psi)\} + \hat{\sigma}_{2,n}^2]^{1/2} \frac{Q_{FDWB,n}^*(\psi)}{[\text{Var}_* \{Q_{FDWB,n}^*(\psi)\}]^{1/2}}, \quad (8)$$

where we first re-scale (7) to have unit variance at the bootstrap level using the bootstrap variance of $Q_{FDWB,n}^*(\psi)$ given by

$$\text{Var}_* \{Q_{FDWB,n}^*(\psi)\} = n^{-1} (4\pi^2)^2 \sum_{\mathbf{j} \in \mathcal{J}_n} \psi(\omega_{\mathbf{j},n}) (\psi(\omega_{\mathbf{j},n}) + \psi(\omega_{-\mathbf{j},n})) \hat{f}_n^2(\omega_{\mathbf{j},n})$$

and then introduce a correction $\text{Var}_* \{Q_{FDWB,n}^*(\psi)\} + \hat{\sigma}_{2,n}^2$ to estimate the correct target variance $\sigma^2 \equiv \sigma_1^2 + \sigma_2^2$; this scaling correction $\text{Var}_* \{Q_{FDWB,n}^*(\psi)\} + \hat{\sigma}_{2,n}^2$ combines the original bootstrap variance $\text{Var}_* \{Q_{FDWB,n}^*(\psi)\}$ as an approximation of the first variance component σ_1^2 , with a subsampling variance estimator $\hat{\sigma}_{2,n}^2 = \hat{\sigma}_n^2 - \hat{\sigma}_{1,n}^2$ from (5) that approximates the second component σ_2^2 . In this

manner, the hybrid bootstrap approximation $H_{HFDB,n}^*(\psi)$ in (8) can capture the correct spread in addition to the shape of the target sampling distribution of $H_n(\psi)$ for spectral inference. In the HFDB method, note that spatial subsampling plays a role in specifically estimating the variance component σ_2^2 that would otherwise be missed by FDWB, while the bootstrap variance $\text{Var}_*\{Q_{FDWB,n}^*(\psi)\}$ from FDWB continues to estimate the first component σ_1^2 as implicit in (7). The next result provides a broad theoretical justification for the HFDB method.

Theorem 4.1. Suppose assumptions of Theorem 3.1 along with (6). Then, for the HFDB version $H_{HFDB,n}^*(\psi)$ of $H_n(\psi)$,

(a) HFDB spread is consistent for the limit variance $\sigma^2 \equiv \sigma_1^2 + \sigma_2^2$ of $H_n(\psi)$:

$$\text{Var}_*\{H_{HFDB,n}^*(\psi)\} = \text{Var}_*\{Q_{FDWB,n}^*(\psi)\} + \widehat{\sigma}_{2,n}^2 \xrightarrow{P} \sigma^2 \text{ as } n \rightarrow \infty.$$

(b) the HFDB approximation is consistent for the target distribution of $H_n(\psi)$:

$$\sup_{x \in \mathbb{R}} \left| P_*(H_{HFDB,n}^*(\psi) \leq x) - P(H_n(\psi) \leq x) \right| \xrightarrow{P} 0 \text{ as } n \rightarrow \infty,$$

where $P_*(\cdot)$ denotes bootstrap probability induced by resampling.

Because the HFDB approach combines bootstrap with spatial subsampling, Theorem 4.1 shows that HFDB achieves consistency for distributional approximations of spectral means statistics under less stringent moment assumptions than previous spatial bootstraps (cf. (Ng, Yau and Chen, 2021)). Furthermore, the methodology presented above for spatial HFDB can then be applied to both Gaussian and non-Gaussian processes, while the original FDWB can only be applied to Gaussian spatial data. Numerical results in Section 5 further demonstrate that the HFDB can perform well, including cases where previous bootstraps approximations (FDWB) can be seen to fail.

Remark 1. As a further observation, we can decompose the target quantity $H_n(\psi)$ as

$$H_n(\psi) \equiv n^{1/2}\{\widehat{M}_n(\psi) - M(\psi)\} = n^{1/2}\{\widehat{M}_n(\psi) - E(\widehat{M}_n(\psi))\} + n^{1/2}\{E(\widehat{M}_n(\psi)) - M(\psi)\},$$

where the first part in the decomposition is a stochastic quantity with mean zero while the second part can be treated as a non-stochastic bias. While the above bias decreases to zero with increasing spatial sample size n , this bias term can potentially impact approximations in small sample sizes. Therefore, in small samples, it is also possible to consider spatial subsampling for estimating this bias part as $\widehat{\text{Bias}}_{\text{sub}} = L^{-1} \sum_{\ell=1}^L b_n^{1/2} (\widehat{M}_{\text{sub}}^{(\ell)}(\psi) - \widehat{M}_n(\psi))$. In which case, we can use $H_{HFDB,n}^* + \widehat{\text{Bias}}_{\text{sub}}$ as a bootstrap approximation to $H_n(\psi)$, which uses subsampling to adjust bootstrap approximations $Q_{FDWB,n}^*(\psi)$ from (7) for both variance as in (8) as well as for bias.

Remark 2. For selecting spatial block size b_n in practice, one may use the *minimum volatility* method as suggested by (Politis, Romano and Wolf, 1999). The idea here is that bootstrap confidence intervals, over an “appropriate” range of block sizes, should remain stable when computed as a function of block size b_n . Using this approach, one can compute bootstrap intervals for a number of block sizes and look for a region where the intervals do not change substantially according to some criterion (e.g., length). One example is to use a procedure based on minimizing a running standard deviation, as suggested by (Politis, Romano and Wolf, 1999). Further, one can also examine a range of block sizes with blocks $\mathcal{D}(n_1^{(b)} \times n_2^{(b)})$ defined by scaling $n_k^{(b)} \approx Cn^{1/4} = C(n_1 n_2)^{1/4}$ for some $C > 0$, which can be an optimal order of spatial subsample size as suggested by (Nordman and Lahiri, 2004).

5. Numerical Studies of Accuracy

In this section, we demonstrate the finite sample performance of the HFDB approximation of spatial spectral statistics. We compare this to the FDWB approximation of (Ng, Yau and Chen, 2021) for spectral mean inference (cf. Section 4) and discuss the relative usefulness of the proposed HFDB method in applications. Note that our theoretical results presented in Section 3 and Section 4 indicate that HFDB should perform well regardless of whether the underlying process is Gaussian or not. That is, HFDB is again intended to remain valid even when the variance component σ_2^2 from (2) is significantly greater than zero, which represents a condition that can be encountered in practice for non-Gaussian data. In cases though where σ_2^2 is exactly zero (as would occur for a Gaussian process) or approximately zero, the HFDB approach is anticipated to perform similarly to FDWB. In the following, we present numerical results for scenarios including a Gaussian process as well as a non-Gaussian process with σ_2^2 differing from zero. To assess the performance of HFDB and FDWB approximations, we consider the coverage accuracy of 90% two-tailed confidence intervals for the covariance parameter $\gamma(\mathbf{h})$ with $\mathbf{h} = (1, 0)^\top$, which are defined as

$$\left(\hat{\gamma}(\mathbf{h}) - \hat{q}_{0.95} n^{-1/2}, \hat{\gamma}(\mathbf{h}) - \hat{q}_{0.05} n^{-1/2} \right),$$

based the sample covariance estimator $\hat{\gamma}(\mathbf{h})$ as a case of a spectral mean statistic. The confidence intervals are constructed using bootstrap quantiles $\hat{q}_{0.05}$ and $\hat{q}_{0.95}$ approximated from 500 Monte Carlo draws for any simulated spatial data set. To estimate the spectral density f in (7) for bootstrap purposes, we used a kernel-based estimator, as detailed in (Crujeiras and Fernandez-Casal, 2010). For each sample size and type of spatial process considered, we performed 1000 Monte Carlo simulations to evaluate coverage and used 500 simulations per simulated dataset to approximate bootstrap distributions. For purposes for understanding the performance of both the FDWB and the HFDB methods in terms of coverage accuracy, below we separate numerical findings by Gaussian and non-Gaussian processes.

5.1. Results for Gaussian processes

For this study, we considered weakly stationary spatial processes with a Matérn covariance function. The parametric model for the spectral density of stationary processes in the Matérn class (cf. (Stein, 1999)) is given by:

$$f(\omega) = \phi(\alpha^2 + \|\omega\|^2)^{-\nu-1},$$

where $\phi > 0$ is a positive constant, α is the inverse of the range parameter, ν is the smoothness parameter, and $\|\cdot\|$ denotes the l_2 norm. For simulations, we have used $\nu = 1$, as this is often a practical choice for many climate applications. The range parameter α and ϕ were controlled to ensure that the process variance is very close to 1, thereby avoiding any nugget variance. This setup allows us to simulate realistic spatial processes and accurately evaluate the performance of our proposed methods. We generated rectangular spatial datasets of sizes 30×30 ($n = 900$), 50×50 ($n = 2500$), and 70×70 ($n = 4900$).

Figure 1 presents the coverage accuracy of 90% two-tailed confidence intervals for the covariance parameter. From Figure 1, we observe that the HFDB and FDWB methods perform similarly for Gaussian processes ($\sigma_2^2 = 0$), as perhaps expected. This similarity is anticipated to occur in this case because HFDB involves a scaling correction to FDWB that is specifically intended to be impactful when σ_2^2 in (2) is non-zero. Moreover, as the overall spatial sample size n increases, the coverage accuracy improves across different range parameters in Figure 1, indicating that both HFDB and FDWB can be effective for Gaussian processes.

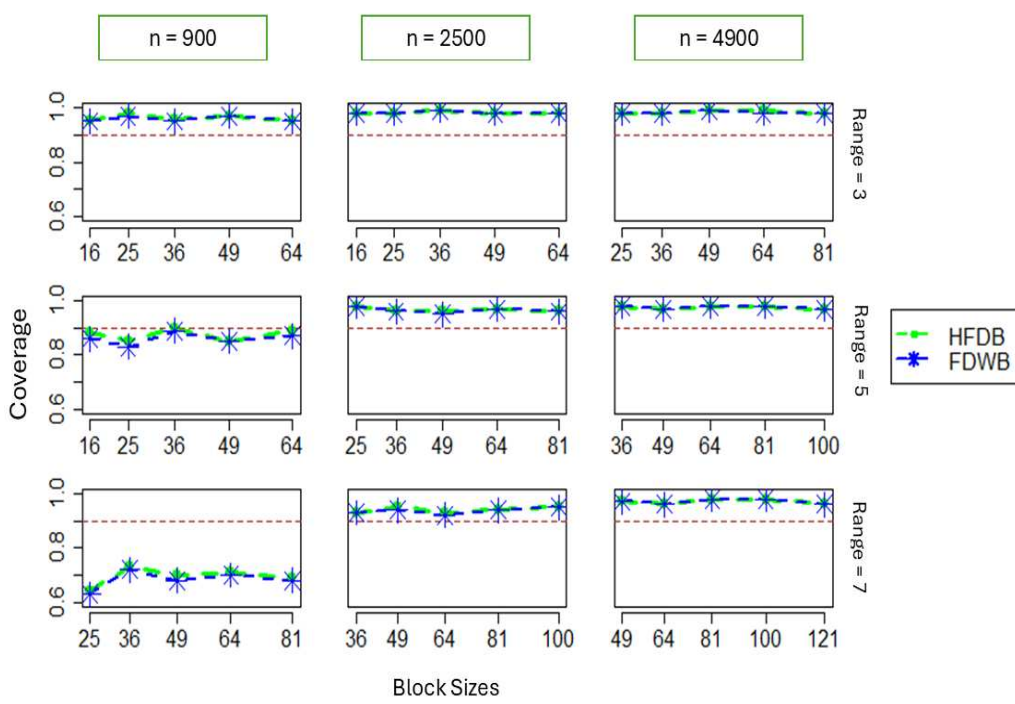


Figure 1. Coverages of 90% HFDB intervals for the covariance parameter $\gamma(\mathbf{h}), \mathbf{h} = (1, 0)^T$, based on either FDWB ($Q_{FDWB,n}^*(\psi)$) (blue line) or corrected ($H_{HFDB,n}^*(\psi)$) (green line) HFDB versions with different sub-sample sizes b_n , range, and sample sizes n .

5.2. Results for non-Gaussian processes

In the non-Gaussian case, we first consider a separable spatial covariance structure by defining a spatial process indexed in the plane as the product of two independent processes indexed in one dimension. This simplification facilitates analysis, providing a clearer understanding of how existing bootstrap methods extend from temporal to spatial settings, particularly with respect to higher-order cumulants and spectral density behavior. Consider two independent weakly stationary time-series $\{X_i\}$ and $\{Y_j\}$ and we generate observation $Z(\mathbf{s}_{i,j})$ at each spatial location $\mathbf{s}_{i,j} = (i, j)$ on a grid $i, j = 1, \dots, \sqrt{n}$ (for $\sqrt{n} = 30, 50, 70$) using $Z(\mathbf{s}_{i,j}) = X_i \cdot Y_j$. In this study, we have used the processes $X_t = 0.2X_{t-1} + \lambda_t$, and $Y_t = -0.7v_{t-1} + v_t$ based on i.i.d innovations $\{\lambda_t\}$ and $\{v_t\}$. Figure 2 presents coverage results under two distributional scenarios for these innovations. The top row of Figure 2 involves innovations λ_t as Gaussian, while v_t follow a standard exponential distribution; the bottom row involves both λ_t and v_t as standard exponential variables. Using the described model, the columns of Figure 2 denote coverages over sample sizes 30×30 ($n = 900$), 50×50 ($n = 2500$), and 70×70 ($n = 4900$).

We note that in Figure 2 the coverage results are based on the bias-corrected HFDB estimator, as described in Remark 1. From this figure, it is evident that the HFDB method significantly outperforms the FDWB estimator in terms of coverage accuracy across all sample sizes, achieving the best coverage across block sizes, and furthermore showing the best coverages as the sample size n increases. The bias correction also helps with smaller sample sizes to achieve improvement in coverages for HFDB. In contrast, the performance of the FDWB deteriorates with increasing sample size. This issue with

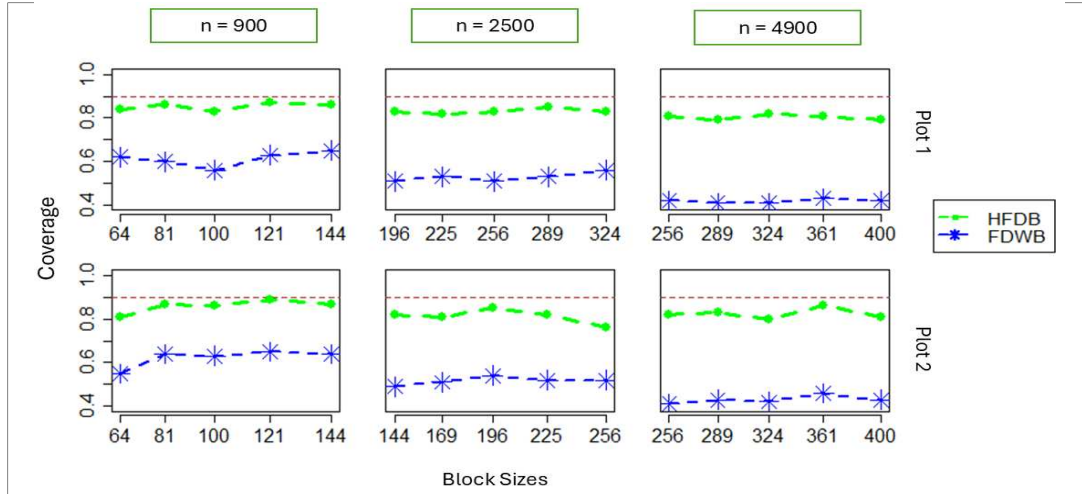


Figure 2. Coverages of 90% HFDB intervals for the covariance parameter $\gamma(\mathbf{h}), \mathbf{h} = (1, 0)^T$, based on either non-corrected ($Q_{FDWB,n}^*(\psi)$) (blue line) or corrected ($H_{HFDB,n}^*(\psi)$) (green line) HFDB versions with different subsample sizes b_n , innovations, and sample sizes n .

the FDWB arises from an incorrect estimation of the limiting variance σ^2 (or σ_2^2 specifically) in (2) so that this bootstrap then leads to incorrect intervals, exhibiting extreme undercoverage in this case involving non-Gaussian processes with non-zero values of σ_2^2 .

We next consider another illustration of coverage accuracy using a non-Gaussian process, which serves to illustrate the behavior of spatial processes found by a nonlinear transformation to a Gaussian process. That is, we first generated a Gaussian process using a Matérn covariance function (cf. (Stein, 1999)), as described earlier in Section 5.1, and applied a quartic transformation of the data to generate a non-Gaussian process which has a positive variance component σ_2^2 . The quartic transformation ensures the resulting process deviates from normality while retaining structured dependence through the underlying Matérn covariance function, allowing for a controlled study of higher-order cumulants (i.e., impacting σ_2^2) and their impact on the frequency domain bootstrap methods.

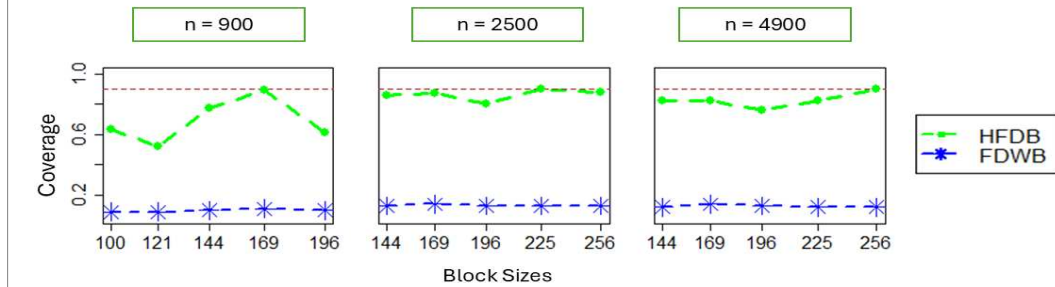


Figure 3. Coverages of 90% HFDB intervals for the covariance parameter $\gamma(\mathbf{h}), \mathbf{h} = (1, 0)^T$, based on either non-corrected ($Q_{FDWB,n}^*(\psi)$) (blue line) or corrected ($H_{HFDB,n}^*(\psi)$) (green line) HFDB versions with different subsample sizes b_n , and sample sizes n .

From Figure 3, we note that the FDWB performs very poorly when the underlying data are from a non-Gaussian distribution here. In contrast, the HFDB consistently outperforms the FDWB across all sample sizes and block sizes. This superior performance of HFDB over FDWB is again due to the fact that the FDWB can fail to capture important variance components in the distribution of spectral mean statistics. By incorporating subsample variance estimation in (8), the HFDB achieves significantly better results than the FDWB and achieves the desired confidence level as the sample size increases.

For non-Gaussian processes with $\sigma_2^2 \approx 0$, our simulation study shows that the performance of both methods are comparable, as may expected in this case. To save space, the detailed results for these cases are presented in the [Supplementary Material](#).

6. Application to Calibrating Spatial Isotropy Tests

Here we examine the performance of bootstrap methods when applied to tests of spatial isotropy (i.e., the covariance function of the stationary spatial process is rotationally invariant). To construct a test, we follow the setup of (Guan, Sherman and Calvin, 2004), which has also been adopted in (Ng, Yau and Chen, 2021). In particular, we consider testing the following hypothesis:

$$H_0 : 2\kappa(\mathbf{h}_i) = 2\kappa(\mathbf{h}_j), \text{ for all } \mathbf{h}_i, \mathbf{h}_j \in \Lambda, \mathbf{h}_i \neq \mathbf{h}_j, \text{ and } \|\mathbf{h}_i\| = \|\mathbf{h}_j\|,$$

where $\Lambda \equiv \{\mathbf{h}_1, \mathbf{h}_2, \dots, \mathbf{h}_m\}$ is a prespecified set of sites and $2\kappa(\mathbf{h}) \equiv E(Z(\mathbf{0}) - Z(\mathbf{h}))^2$ is the variogram at lag \mathbf{h} ; also above $\|\mathbf{h}\| \equiv \sqrt{\mathbf{h}^T \mathbf{h}}$. This null hypothesis can also be written in terms of a spectral mean assessment of whether $M(\psi) = 0$ holds for various spectral mean parameterized defined by $\psi(\omega) \equiv \{2\cos(\mathbf{h}_j^T \omega) - 2\cos(\mathbf{h}_i^T \omega)\}$. Letting $G \equiv (2\kappa(\mathbf{h}_1), \dots, 2\kappa(\mathbf{h}_m))$ denote a vector of variograms in Λ , it holds that, under H_0 , there exists a full row rank matrix A such that $AG = 0$. For example, if $\Lambda = \{(1, 0), (0, 1)\}$, then $G = (2\kappa(1, 0), 2\kappa(0, 1))$, and we may set $A = \begin{bmatrix} 1 & -1 \end{bmatrix}$. Exploiting this property, (Guan, Sherman and Calvin, 2004) proposed a test statistic $TS_n \equiv n \times (A\hat{G}_n)^T (A\hat{\Sigma}_R A^T)^{-1} (A\hat{G}_n)$, where \hat{G}_n is the vector of sample variogram estimates at lag $\mathbf{h} \in \Lambda$, n is number of locations, and $\hat{\Sigma}_R$ is an estimator of the covariance matrix Σ_R of sample variograms. Under H_0 , (Guan, Sherman and Calvin, 2004) derived that $TS_n \xrightarrow{D} \chi_k^2$ as $n \rightarrow \infty$, where k is the row rank of A . Due to the slow convergence of the test statistic, (Guan, Sherman and Calvin, 2004) further considered a subsampling method to determine the p-value of the test. However, since this test statistic involves spectral mean statistics in the form of variogram (or related covariance) estimators, we may study the proposed bootstrap approach in HFDB for approximating the p-values of the test.

For purposes of simulating spatial data to examine size control and power in testing, we use a mean zero Gaussian process with a spherical covariance function,

$$\gamma(\mathbf{h}) \equiv \begin{cases} \sigma^2 \left(1 - \frac{3r}{2\phi} + \frac{r^3}{2\phi^3} \right) + \eta \mathbb{I}\{\mathbf{h} = \mathbf{0}\} & \text{if } 0 \leq r \leq \phi, \\ \eta \mathbb{I}\{\mathbf{h} = \mathbf{0}\} & \text{otherwise,} \end{cases} \quad (9)$$

where σ^2 is the partial sill parameter, ϕ is the range parameter, η is the nugget effect, and $r \equiv \sqrt{\mathbf{h}^T B \mathbf{h}}$ is a distance related to a matrix B , described next, as geometric anisotropy transformation. Given an anisotropy angle τ_A and anisotropy ratio τ_R , define the rotation matrix R and shrinking matrix T as

$$R \equiv \begin{bmatrix} \cos(\tau_A) & \sin(\tau_A) \\ -\sin(\tau_A) & \cos(\tau_A) \end{bmatrix} \text{ and } T \equiv \begin{bmatrix} 1 & 0 \\ 0 & \tau_R \end{bmatrix},$$

then we may set $B \equiv R' T' T R$ is a 2×2 positive definite matrix representing a geometric anisotropy transformation. A random field with spherical covariance function as in (9) is called generally anisotropic unless $\tau_R = 1$ holds, which corresponds to the isotropic case. Also, if $\tau_A = 0$ holds, then the main anisotropic axes are aligned with the the standard coordinate axes (x, y) in the plane making $\tau_A = 0$ as a helpful choice in interpretation.

In particular, we consider the model parameters $(\eta, \sigma^2, \phi, \tau_A, \tau_R) = (0, 1, 5, 0, \tau_R)$ for different anisotropy ratio τ_R . Also, we set $\Lambda = \{\mathbf{h}_1, \mathbf{h}_2\}$ for $\mathbf{h}_1 \equiv (1, 0)$ and $\mathbf{h}_2 \equiv (0, 1)$ along with $G = (2\kappa(\mathbf{h}_1), 2\kappa(\mathbf{h}_2))^T$, and $A = \begin{bmatrix} 1 & -1 \end{bmatrix}$ so that the test statistic form may be written as $TS_n \equiv n \times [2\hat{\kappa}(\mathbf{h}_1) - 2\hat{\kappa}(\mathbf{h}_2)]^2 (A \hat{\Sigma}_R A^T)^{-1}$, where $\hat{\kappa}(\mathbf{h}_i)$, $i = 1, 2$, are sample variograms and where $\hat{\Sigma}_R$ may be determined by subsampling or some other device. However, since $(A \hat{\Sigma}_R A^T)^{-1}$ is only a real-valued factor, we may consider a related, but simpler, test statistic $TS_n = n \times (2\hat{\kappa}(1, 0) - 2\hat{\kappa}(0, 1))^2 = n \hat{M}_n^2(\psi)$ to assess the null hypothesis of isotropy, which involves examining the square $\hat{M}_n^2(\psi)$ of a spectral mean statistic $\hat{M}_n(\psi)$ based on $\psi(\omega) \equiv \{2\cos(\mathbf{h}_1^T \omega) - 2\cos(\mathbf{h}_2^T \omega)\}$ that should be near zero under isotropy. To consider different resampling approximations for calibrating this test statistic, we examine subsampling as in (Guan, Sherman and Calvin, 2004) as well as FDWB from (Ng, Yau and Chen, 2021), and the proposed HFDB here. Both FDWB and HFDB versions of this test statistic are computed as $[Q_{FDWB,n}^*(\psi)]^2$ and $[H_{HDWB,n}^*(\psi)]^2$, respectively, upon applying $\psi(\omega) \equiv \{2\cos(\mathbf{h}_1^T \omega) - 2\cos(\mathbf{h}_2^T \omega)\}$ in (7) and (8); note that bootstrap statistics are then centered to have mean zero which mimics how $[H_n(\psi) \equiv \sqrt{n}(\hat{M}_n(\psi) - M_n(\psi))]$ behaves under null hypothesis with $M_n(\psi) = 0$.

In the simulation study, we have used the spherical covariance function as in (9) to generate a mean-zero Gaussian spatial process, following (Guan, Sherman and Calvin, 2004) and (Ng, Yau and Chen, 2021). To construct a mean-zero non-Gaussian spatial process, we use the Matérn covariance with parameters $(\alpha, \nu) = (1/3, 1)$, as described in Section 5.1. Specifically, we generate the field by multiplying the Cholesky factor of the covariance matrix with a vector of standard exponential random variables shifted to have mean zero, thereby introducing non-Gaussianity while preserving the desired spatial dependence structure.

Tables 1-2 display observed rejection probabilities (based on 1000 simulations) for the Gaussian and non-Gaussian processes, respectively, based on sample sizes of 50×50 with a nominal testing level of 10%; similar results for a sample region 30×30 are presented in [Supplementary Material](#) to save space. We have used block sizes of 9×9 for the Gaussian process and 5×5 for the non-Gaussian processes to account for differences in spatial dependence and marginal behavior. The larger block size captures the smoother structure of Gaussian data, while the smaller size helps preserve the features, such as skewness and heavy tails. Table 1 demonstrates that all methods perform well when the underlying distribution is Gaussian, and both FDWB and HFDB perform similarly. In particular, both maintain size close to the nominal level of 10% when the null hypothesis of isotropy is true (i.e., $\tau_R = 1$), and both show increasing power as τ_R deviates from 1. However, under non-Gaussianity, FDWB fails to maintain size under isotropy to the extent that this is unsuitable for power comparison under non-Gaussian scenarios in Table 2. In contrast, both HFDB and subsampling remain effective under non-Gaussianity, with HFDB showing some advantage over subsampling as the anisotropy ratio increases.

Table 1. Rejection rates for Gaussian data.

τ_R	Subsampling	FDWB	HFDB
1	0.084	0.103	0.103
1.1	0.135	0.223	0.223
1.2	0.424	0.537	0.537
1.3	0.787	0.88	0.88
1.4	0.912	0.983	0.983
1.5	0.996	1	1

Table 2. Rejection rates for Non-Gaussian data.^a

τ_R	Subsampling	HFDB
1	0.078	0.1
1.2	0.112	0.17
1.3	0.391	0.497
1.4	0.693	0.77
1.5	0.907	0.972
1.6	0.993	1

^aFor non-Gaussian data, FDWB fails to maintain the size at the 10% level, with a rejection rate of 0.243 for $\tau_R = 1$; this bootstrap becomes inappropriate for non-Gaussian data and is so excluded from Table 2.

7. Concluding Remarks

The proposed spatial resampling method, called Hybrid Frequency Domain Bootstrap (HFDB), combines two resampling approaches in the form of subsampling and bootstrap in order to validly approximate the distribution of spatial spectral mean statistics. Spectral means are fundamental spatial parameters, yet spectral statistics have complicated distributions owing to complex variances that are difficult to estimate. Previous bootstrap methods, such as the FDWB proposed by (Ng, Yau and Chen, 2021), rely on specific distributional assumptions and can fail to provide valid distributional approximations for non-Gaussian spatial data, due to issues in correctly capturing the variances of spectral statistics for such data. In contrast, the HFDB overcomes these limitations by incorporating a scaling adjustment from spatial subsampling to correct the spread of bootstrap approximations in the frequency domain. This leads to more accurate and general estimation of the sampling distribution of spatial spectral mean statistics.

The numerical results in Sections 5-6 illustrate the finite-sample performance of the HFDB method in terms of testing and interval estimation, while the theoretical results in Sections 3-4 provide some formal guarantees of consistency in HFDB distributional approximations. Importantly, our results hold under mild spatial conditions, which allows a broad scope of application for applying HFDB to spectral problems of assessing spatial covariance structure, with both Gaussian and non-Gaussian spatial processes. Main results along with further technical results on establishing subsampling and bootstrap for spatial data are provided in the Appendix.

Appendix

For notational simplicity b will be used instead of b_n in the following proofs. All proofs are performed within the framework outlined in Section 2. Now, to prove Theorem 3.1 and Theorem 4.1 we will use the following lemmas which summarize all the subsampling results for spectral means that are used repeatedly in later proofs. Define $G^*(\omega_{j,n}) := \widehat{f}_n(\omega_{j,n})U_j^*$, where U_j^* s are i.i.d standard exponential drawn using the exponential resampling mechanism. We begin by presenting the lemmas and proposition necessary for proving the theorems. The proofs of the lemmas are provided last.

Lemma A.1. Suppose Assumptions 1-3 hold for a generic function $\psi : \Pi^2 \rightarrow \mathbb{R}$ of bounded variation with $H_n(\psi) \equiv n^{1/2}\{\widehat{M}_n(\psi) - M(\psi)\} \xrightarrow{D} \mathcal{N}(0, \sigma^2)$, where $\widehat{M}_n(\psi)$, $M(\psi)$, and σ^2 are defined analogously as in Section 2.2 and Section 2.3. Then if subsample size b satisfies $1/n_k^{(b)} + n_k^{-1}n_k^{(b)} \rightarrow 0$ for $k = 1, 2$ as $n \rightarrow \infty$,

- (i) $\sup_{x \in \mathbb{R}} \left| L^{-1} \sum_{l=1}^L \mathbb{I}\{b^{1/2}(\widehat{M}_{\text{sub}}^{(\ell)}(\psi) - M(\psi)) \leq x\} - P(H_n(\psi) \leq x) \right| \xrightarrow{P} 0;$
- (ii) $\sup_{x \in \mathbb{R}} \left| L^{-1} \sum_{l=1}^L \mathbb{I}\{b^{1/2}(\widehat{M}_{\text{sub}}^{(\ell)}(\psi) - \widetilde{M}_n(\psi)) \leq x\} - P(H_n(\psi) \leq x) \right| \xrightarrow{P} 0;$
- (iii) $b^{1/2}(\widetilde{M}_n(\psi) - M(\psi)) \xrightarrow{P} 0;$
- (iv) $L^{-1} \sum_{l=1}^L b(\widehat{M}_{\text{sub}}^{(\ell)}(\psi) - M(\psi))^2 \xrightarrow{P} \sigma^2(\psi);$
- (v) $L^{-1} \sum_{l=1}^L b(\widehat{M}_{\text{sub}}^{(\ell)}(\psi) - \widetilde{M}_n(\psi))^2 \xrightarrow{P} \sigma^2(\psi),$

where $\widehat{M}_{\text{sub}}^{(\ell)}(\psi)$, and $\widetilde{M}_n(\psi)$ are analogously defined as in Section 3.1.

Lemma A.2. Suppose Assumptions 1-3 and 4 hold. Then for a generic function $\psi : \Pi^2 \rightarrow \mathbf{R}$ of bounded variation, if the subsample length b satisfies $1/n_k^{(b)} + n_k^{-1}n_k^{(b)} \rightarrow 0$ for $k = 1, 2$ as $n \rightarrow \infty$ then,

$$4\pi^2 b^{-1} \sum_{\mathbf{j} \in \mathcal{J}_b} \psi(\omega_{\mathbf{j},b}) L^{-1} \sum_{\ell=1}^L \left(\mathcal{I}_{\text{sub}}^{(\ell)}(\omega_{\mathbf{j},b}) - \widetilde{\mathcal{I}}_n(\omega_{\mathbf{j},b}) \right)^2 \xrightarrow{P} \int_{\Pi^2} \psi(\omega) f^2(\omega) d\omega.$$

Proposition A.3. For $Q_{FDWB,n}^*(\psi)$, and $\sigma_1^2(\psi)$ as defined in Section 4, and Section 2.3 the following are true.

- (i) $\text{Var}_*\{Q_{FDWB,n}^*(\psi)\} \xrightarrow{P} \sigma_1^2(\psi);$
- (ii) $\sup_{x \in \mathbb{R}} \left| P_*(Q_{FDWB,n}^*(\psi) \leq x) - \Phi(x/\sigma_1(\psi)) \right| = o_P(1),$

where P_* is the probability distribution induced by resampling, Var_* is the resampled variance, and $\Phi(\cdot)$ is the standard normal distribution function.

Proof of Proposition A.3.

By the exponential resampling mechanism, we have $\text{Cov}_*(U_{\mathbf{j}}^*, U_{\mathbf{k}}^*) = \mathbb{I}\{\mathbf{j} = -\mathbf{k}\}$. Hence, with \widehat{f}_n being an even function it follows, $\text{Cov}_*(G^*(\omega_{\mathbf{j},n}), G^*(\omega_{\mathbf{k},n})) = \widehat{f}_n^2(\omega_{\mathbf{j},n}) \mathbb{I}\{\mathbf{j} = -\mathbf{k}\}$ and,

$$\begin{aligned} \text{Var}_*(Q_{FDWB,n}^*(\psi)) &= \frac{(4\pi^2)^2}{n} \sum_{\mathbf{j}, \mathbf{k} \in \mathcal{J}_n} \psi(\omega_{\mathbf{j},n}) \psi(\omega_{\mathbf{k},n}) \text{Cov}_*(G^*(\omega_{\mathbf{j},n}), G^*(\omega_{\mathbf{k},n})) \\ &= (2\pi)^2 \sum_{\mathbf{j} \in \mathcal{J}_n} \frac{(2\pi)^2}{n} \psi(\omega_{\mathbf{j},n}) \{\psi(\omega_{\mathbf{j},n}) + \psi(\omega_{-\mathbf{j},n})\} f^2(\omega_{\mathbf{j},n}) \\ &\quad + \frac{(4\pi^2)^2}{n} \sum_{\mathbf{j} \in \mathcal{J}_n} \psi(\omega_{\mathbf{j},n}) \{\psi(\omega_{\mathbf{j},n}) + \psi(\omega_{-\mathbf{j},n})\} (\widehat{f}_n^2(\omega_{\mathbf{j},n}) - f^2(\omega_{\mathbf{j},n})) \\ &=: S_1 + S_2 \end{aligned}$$

Since, S_1 is a Riemann sum, it immediately follows that $S_1 = \sigma_1^2(\psi) + O(1)$. Using $|\mathcal{J}_n| = O(n)$ and Eq. (6) we have $S_2 = o_P(1)$ which completes the proof of A.3(i).

For notational ease, we define $\mathcal{J}_n^+ \equiv \{\mathbf{j} \equiv (j_1, j_2) \in \mathcal{J}_n : \text{either } j_1 > 0 \text{ or } j_1 = 0 \text{ and } j_2 > 0\}$. Since $\{U_{\mathbf{j}}^*, \mathbf{j} \in \mathcal{J}_n^+\}$ are i.i.d standard exponentially distributed and $U_{\mathbf{j}}^* \equiv U_{-\mathbf{j}}^*$ for $\mathbf{j} \in \mathcal{J}_n$ where $-\mathbf{j} \in \mathcal{J}_n^+$,

then $Q_{FDWB,n}^*(\psi)$ can be written as

$$Q_{FDWB,n}^* = n^{-1/2} \sum_{\mathbf{j} \in \mathcal{J}_n^+} V_{\mathbf{j},n}^*, \quad (10)$$

where,

$$V_{\mathbf{j},n}^* = (2\pi)^2 (\psi(\omega_{\mathbf{j},n}) \widehat{f}_n(\omega_{\mathbf{j},n}) + \psi(-\omega_{\mathbf{j},n}) \widehat{f}_n(-\omega_{\mathbf{j},n})) (U_{\mathbf{j}}^* - 1), \quad \mathbf{j} \in \mathcal{J}_n^+.$$

Since, $|\mathcal{J}_n^+| \rightarrow \infty$, as $n \rightarrow \infty$, a conditional version of Lyapunov's CLT can be applied to Eq. (10) (using the established convergence in probability of $\text{Var}_*(Q_{FDWB,n}^*(\psi))$ to a positive constant from (i)), i.e., we have to find a $\nu > 0$ such that

$$n^{-(1+\nu/2)} \sum_{\mathbf{j} \in \mathcal{J}_n^+} E^* \left(|V_{\mathbf{j},n}^*|^{2+\nu} \right) = o_P(1). \quad (11)$$

Choosing $\nu = 1$, we have

$$\sum_{\mathbf{j} \in \mathcal{J}_n^+} |\psi(\omega_{\mathbf{j},n}) \widehat{f}_n(\omega_{\mathbf{j},n}) + \psi(-\omega_{\mathbf{j},n}) \widehat{f}_n(-\omega_{\mathbf{j},n})| \leq n \cdot \sup_{\omega \in \Pi} |\psi(\omega)| \cdot \sup_{\omega \in \Pi} |\widehat{f}_n(\omega)| = O_P(n),$$

since both ψ and f (due to absolutely summable autocovariance function) are bounded, and due to Eq. (6). Hence, it holds that

$$\sum_{\mathbf{j} \in \mathcal{J}_n^+} \left| \psi(\omega_{\mathbf{j},n}) \widehat{f}_n(\omega_{\mathbf{j},n}) + \psi(-\omega_{\mathbf{j},n}) \widehat{f}_n(-\omega_{\mathbf{j},n}) \right|^3 = O_P(n). \quad (12)$$

Since, $U_{\mathbf{j}}^*$ are standard exponential we have $E^*(|U_{\mathbf{j}}^* - 1|^3) = 12e^{-1} - 2 = K$ (Say) gives us

$$\sum_{\mathbf{j} \in \mathcal{J}_n^+} E^* \left(|V_{\mathbf{j},n}^*|^{2+\nu} \right) = (4\pi^2)^3 K \sum_{\mathbf{j} \in \mathcal{J}_n^+} \left| \psi(\omega_{\mathbf{j},n}) \widehat{f}_n(\omega_{\mathbf{j},n}) + \psi(-\omega_{\mathbf{j},n}) \widehat{f}_n(-\omega_{\mathbf{j},n}) \right|^3 = O_P(n),$$

due to Eq. (12). This shows Lyapunov condition holds for Eq. (11) when $\nu = 1$. Together with A.3(i), the assertion in A.3(ii) follows. \square

Proof of Theorem 3.1

Using Lemma A.2, we have $\widehat{\sigma}_{1,n}^2(\psi) \xrightarrow{P} \sigma_1^2(\psi)$. Since, $\psi(\cdot)$ is of bounded variation, so is $\psi(\omega)(\psi(\omega) + \psi(-\omega))$. Using Slutsky's theorem and Lemma A.1(v) we have $\widehat{\sigma}_{2,n}^2(\psi) = \widehat{\sigma}_n^2(\psi) - \widehat{\sigma}_{1,n}^2(\psi) \xrightarrow{P} \sigma^2(\psi) - \sigma_1^2(\psi) = \sigma_2^2(\psi)$. Then the statement of Theorem 3.1 follows from (v). \square

Proof of Theorem 4.1

(a) Now Proposition A.3(i) and Slutsky's theorem gives us $\text{Var}_*\{Q_{FDWB,n}^*(\psi)\} + \widehat{\sigma}_{2,n}^2(\psi) \xrightarrow{P} \sigma^2(\psi)$, which completes the proof.

(b) Next we prove the consistency of the distribution of the HFDB estimator. Consider an arbitrary sequence $\{n_m\}$ of $\{n\}$. Then it follows from Proposition A.3 (i) and (ii) that there exists a further

subsequence $\{n_{m_k}\}$ of $\{n_m\}$ such that,

$$\sup_{x \in \mathbb{R}} \left| P_*(Q_{FDWB, n_{m_k}}^*(\psi) \leq x) - \Phi(x/\sigma_1(\psi)) \right| \xrightarrow{a.s.} 0; \quad \text{Var}_*\{Q_{FDWB, n_{m_k}}^*(\psi)\} \xrightarrow{a.s.} \sigma_1^2(\psi).$$

It follows from Corollary 3.1(b) that $\text{Var}_*\{Q_{FDWB, n_{m_k}}^*(\psi)\} + \widehat{\sigma}_{2, n_{m_k}}^2(\psi) \xrightarrow{a.s.} \sigma^2(\psi)$ as $n_{m_k} \rightarrow \infty$. Now, along the subsequence $\{n_{m_k}\}$ we have $Q_{FDWB, n_{m_k}}^*(\psi) \xrightarrow{D} \mathcal{N}(0, \sigma_1^2(\psi))$. Thus, using Slutsky's theorem gives us $H_{HFDB, n_{m_k}}^*(\psi) \xrightarrow{D} \mathcal{N}(0, \sigma^2(\psi))$. Therefore, we have

$$\sup_{x \in \mathbb{R}} \left| P_*(H_{HFDB, n_{m_k}}^*(\psi) \leq x) - \Phi(x/\sigma(\psi)) \right| \xrightarrow{a.s.} 0$$

as $n_{m_k} \rightarrow \infty$. Since the choice of the sub-sequence is arbitrary, we have

$$\sup_{x \in \mathbb{R}} \left| P_*(H_{HFDB, n}^*(\psi) \leq x) - \Phi(x/\sigma(\psi)) \right| \xrightarrow{P} 0, \quad \text{as } n \rightarrow \infty.$$

Now using $\sup_{x \in \mathbb{R}} |P(H_n(\psi) \leq x) - \Phi(x/\sigma(\psi))| = o_P(1)$ and triangle inequality we have,

$$\sup_{x \in \mathbb{R}} \left| P_*(H_{HFDB, n}^*(\psi) \leq x) - P(H_n(\psi) \leq x) \right| \xrightarrow{P} 0 \quad \text{as } n \rightarrow \infty$$

which completes the proof. \square

Proof of Lemma A.1

To formalize our proofs, we introduce the following: for $r = 1, 2$, and $x \in \mathbb{R}$,

$$H_n \equiv H_n(\psi); \quad Y \sim \mathcal{N}(0, \sigma^2(\psi)), \quad t_n^{(r)} \equiv E(H_n^r), \quad t_{n,C}^{(r)} \equiv E(H_n - E(H_n))^r,$$

$$F_n(x) \equiv P(H_n \leq x), \quad F(x) \equiv P(Y \leq x),$$

$$\widehat{F}_n(x) \equiv L^{-1} \sum_{\ell=1}^L \mathbb{I}[b_n^{1/2}(\widehat{M}_{\text{sub}}^{(\ell)}(\psi) - M(\psi)) \leq x]; \quad \widehat{F}_{n,C}(x) \equiv L^{-1} \sum_{\ell=1}^L \mathbb{I}[b_n^{1/2}(\widehat{M}_{\text{sub}}^{(\ell)}(\psi) - \widetilde{M}_n(\psi)) \leq x];$$

$$\widehat{t}_n^{(r)} \equiv L^{-1} \sum_{\ell=1}^L \left\{ b_n^{1/2} \left(\widehat{M}_{\text{sub}}^{(\ell)}(\psi) - M(\psi) \right) \right\}^r; \quad \widehat{t}_{n,C}^{(r)} \equiv L^{-1} \sum_{\ell=1}^L \left\{ b_n^{1/2} \left(\widehat{M}_{\text{sub}}^{(\ell)}(\psi) - \widetilde{M}_n(\psi) \right) \right\}^r.$$

These definitions establish key quantities used to prove the asymptotic validity of bootstrap procedures. They distinguish between population-level targets (e.g., $M(\psi)$) and sample-based estimates (e.g., $\widetilde{M}_n(\psi)$) to carefully track bias and variability in the resampling framework. We define r -th order central moments and empirical distributions centered around both the true and estimated targets.

First we prove statement A.1(i). By notation defined above, we have to show $\sup_{x \in \mathbb{R}} |\widehat{F}_n(x) - F(x)| \xrightarrow{P} 0$ as $n \rightarrow \infty$. Let $C \subset \mathbb{R}$ is the set of continuity points of F . It suffices to show $\widehat{F}_n(x_0) \xrightarrow{P} F(x_0)$ as $n \rightarrow \infty$ for an arbitrary fixed $x_0 \in C$. From this, one may take a countable, dense(in \mathbb{R}) collection $\{x_i : i \geq 1\} \subset C$ and, for any sub-sequence $\{n_m\}$ of $\{n\}$, extract a further sub-sequence $\{n_{m_k}\} \equiv \{n_k\}$ where, almost surely(a.s.), it holds that $\widehat{F}_{n_{m_k}}(x_i) \rightarrow F(x_i)$ as $n_{m_k} \rightarrow \infty$ for each $i \geq 1$; the latter implies that $\sup_{x \in \mathbb{R}} |\widehat{F}_{n_{m_k}}(x) - F(x)| \xrightarrow{a.s.} 0$, which is equivalent to $\sup_{x \in \mathbb{R}} |\widehat{F}_n(x) - F(x)| \xrightarrow{P} 0$ as $\{n_m\}$ was arbitrary. Then statement (i) follows from a triangle inequality.

Now, due to boundedness, $\widehat{F}_n(x_0) \xrightarrow{P} F(x_0)$ is equivalent to $E(\widehat{F}_n(x_0) - F(x_0))^2 \rightarrow 0$, and we show the latter.

To control this, fix $\lambda \in (0, 1)$ where λ sets a threshold for spatial proximity, and for $\mathbf{j} = (j_1, j_2), \mathbf{k} = (k_1, k_2)$ integer vectors in the plane (the i -th component can be $0, 1, \dots, (n_i - n_i^{(b)})$ for $i = 1, 2$) we split the double sum of covariances in the MSE into indices \mathbf{j}, \mathbf{k} such that:

- (a) $|j_i - k_i| < \lambda n_i$ for some $i = 1, 2$,
- (b) and those for which $|j_i - k_i| \geq \lambda n_i$ for both $i = 1, 2$.

In case (a), the number of such dependent index pairs has an upper bound $n\lambda/L$.

In case (b), the assumption

$$\frac{|j_i - k_i|}{n_i^{(b)}} \rightarrow \infty \quad \text{for } i = 1, 2,$$

along with $n_i^{(b)}/n_i \rightarrow 0$ (or $n_i/n_i^{(b)} \rightarrow \infty$), implies that the covariance between $\mathbb{I}(H_{\mathbf{j},b} \leq x_0)$ and $\mathbb{I}(H_{\mathbf{k},b} \leq x_0)$ must disappear asymptotically. That is,

$$\begin{aligned} & \sup_{\substack{|j_i - k_i| \geq \lambda n_i \\ \forall i=1,2}} \text{Cov}(\mathbb{I}(H_{\mathbf{j},b} \leq x_0), \mathbb{I}(H_{\mathbf{k},b} \leq x_0)) \\ &= \sup_{\substack{|j_i - k_i| \geq \lambda n_i \\ \forall i=1,2}} |P(H_{\mathbf{j},b} \leq x_0, H_{\mathbf{k},b} \leq x_0) - P(H_{\mathbf{j},b} \leq x_0)P(H_{\mathbf{k},b} \leq x_0)| \rightarrow 0, \end{aligned}$$

by Assumption 3. This guarantees

$$D_{1,n}(\lambda) := \sup_{\substack{|j_i - k_i| \geq \lambda n_i \\ \forall i=1,2}} |P(H_{\mathbf{j},b} \leq x_0, H_{\mathbf{k},b} \leq x_0) - F(x_0)^2| \rightarrow 0,$$

$$D_{2,n}(\lambda) := \sup_{\substack{j_i \in \{0, 1, \dots, (n_i - n_i^{(b)})\} \\ \forall i=1,2}} |P(H_{\mathbf{j},b} \leq x_0) (F(x_0) - P(H_{\mathbf{j},b} \leq x_0))| \rightarrow 0.$$

Combining, we obtain:

$$E \left(\widehat{F}_n(x_0) - F(x_0) \right)^2 \leq \frac{n\lambda}{L} + D_{1,n}(\lambda) + D_{2,n}(\lambda) \rightarrow \lambda.$$

Since $\lambda > 0$ is arbitrary, we conclude:

$$E \left(\widehat{F}_n(x_0) - F(x_0) \right)^2 \rightarrow 0,$$

completing the proof of Lemma A.1(i).

Next, we prove statements (iii) - (v) together. First we would like to prove the following statements: if $\lim_{n \rightarrow \infty} E(H_{\mathbf{j}^{(n)},n}^2) = E(Y^2)$ hold for any vector of integer sequence $\mathbf{j}^{(n)}$, then

$$\widehat{t}_n^{(1)} \xrightarrow{P} t_n^{(1)}, \quad \widehat{t}_n^{(2)} \xrightarrow{P} t_n^{(2)}, \quad \text{and} \quad \widehat{t}_{n,C}^{(2)} \xrightarrow{P} t_{n,C}^{(2)} \quad \text{as } n \rightarrow \infty. \quad (13)$$

We show $\widehat{t}_n^{(r)} \xrightarrow{P} t_n^{(r)}$, for $r = 1, 2$. We would also have $\widehat{t}_{n,C}^{(2)} \xrightarrow{P} t_{n,C}^{(2)}$ by Slutsky's theorem.

For any $C > 0$ such that $\pm C \in C$, it follows from statement (i) that

$$\widehat{t}_n^{(r)}(C) \equiv \frac{1}{L} \sum_{\ell=1}^L H_{\mathbf{j}^{(\ell)},b}^r \mathbb{I}\{|H_{\mathbf{j}^{(\ell)},b}| \leq C\} = \int y^r \mathbb{I}\{|y| \leq C\} d\widehat{F}_n(y) \xrightarrow{P} E(Y^r \mathbb{I}\{|Y| \leq C\}). \quad (14)$$

That is, by statement (i), for any sub-sequence $\{n_j\}$ of $\{n\}$, there exists again further sub-sequence $\{n_k\} \subset \{n_j\}$ where $\sup_{x \in \mathbb{R}} |\widehat{F}_{n_k}(x) - F(x)| \xrightarrow{a.s.} 0$ as $\{n_k\} \rightarrow \infty$. Then using Continuous Mapping theorem, for a random variable $Y_{n_k}^* \sim \widehat{F}_{n_k}$, we have $(Y_{n_k}^*)^r \mathbb{I}\{|Y_{n_k}^*| \leq C\} \xrightarrow{D} Y^r \mathbb{I}\{|Y| \leq C\}$, and so the corresponding expected values (bounded) converge as $\int y^r \mathbb{I}\{|y| \leq C\} d\widehat{F}_{n_k}(y) \xrightarrow{a.s.} E(Y^r \mathbb{I}\{|Y| \leq C\})$ as $n_k \rightarrow \infty$ implying Eq. (14). For given $\nu > 0$ and $\lambda \in (0, 1)$, pick and fix C such that $E(Y^r \mathbb{I}\{|Y| > C\}) < \nu\lambda/3$. Then it suffices to show

$$\limsup_{n \rightarrow \infty} P\left(\left|\widehat{t}_n^{(r)} - \widehat{t}_n^{(r)}(C)\right| > \nu/3\right) \leq \lambda, \quad (15)$$

from which

$$\begin{aligned} \limsup_{n \rightarrow \infty} P\left(\left|\widehat{t}_n^{(r)} - E(Y^r)\right| > \nu\right) &\leq \limsup_{n \rightarrow \infty} P\left(\left|\widehat{t}_n^{(r)}(C) - E(Y^r \mathbb{I}\{|Y| \leq C\})\right| > \nu/3\right) \\ &\quad + \limsup_{n \rightarrow \infty} P\left(\left|\widehat{t}_n^{(r)} - \widehat{t}_n^{(r)}(C)\right| > \nu/3\right) \leq \lambda \end{aligned}$$

follows by Eq. (14)-(15) and $P(E(Y^r \mathbb{I}\{|Y| > C\}) > \nu/3) = 0$, which gives us $\widehat{t}_n^{(r)} \xrightarrow{P} E(Y^r)$. Since we have assumed for any vector of integer sequence $\mathbf{j}^{(n)}$, $E(H_{\mathbf{j}^{(n)}, n}^2) \rightarrow E(Y^2)$ as $n \rightarrow \infty$, we have $t_n^{(2)} \equiv E(H_n^2) \rightarrow E(Y^2) = \sigma^2(\psi)$ and, by dominated convergence theorem (DCT), $E(|H_n|) \rightarrow E(|H|)$ and $t_n^{(1)} \equiv E(H_n) \rightarrow E(Y) = 0$ as $n \rightarrow \infty$. Thus, we have established $\widehat{t}_n^{(r)} \xrightarrow{P} t_n^{(r)}$ for $r = 1, 2$.

By Markov's inequality, for $r = 1, 2$, we have

$$P\left(\left|\widehat{t}_n^{(r)} - \widehat{t}_n^{(r)}(C)\right| > \nu/3\right) \leq \frac{\nu}{3} \max_{1 \leq \ell \leq L} E\left(|H_{\mathbf{j}^{(\ell)}, b}|^r \mathbb{I}\{|H_{\mathbf{j}^{(\ell)}, b}| > C\}\right),$$

so that, Eq. (15) follows from $\limsup_{n \rightarrow \infty} \max_{1 \leq \ell \leq L} E\left(|H_{\mathbf{j}^{(\ell)}, b}|^r \mathbb{I}\{|H_{\mathbf{j}^{(\ell)}, b}| > C\}\right) \leq \nu\lambda/3$ which is implied by the moment conditions. Note that a contrary result

$$\limsup_{n \rightarrow \infty} \max_{1 \leq \ell \leq L} E\left(|H_{\mathbf{j}^{(\ell)}, b}|^r \mathbb{I}\{|H_{\mathbf{j}^{(\ell)}, b}| > C\}\right) > \nu\lambda/3$$

would imply existence of a sub-sequence $\{n_j\}$ and a positive integer m_{n_j} such that

$$E\left(|H_{\mathbf{j}^{(m_{n_j})}, b_{n_j}}|^r \mathbb{I}\{|H_{\mathbf{j}^{(m_{n_j})}, b_{n_j}}| > C\}\right) > \nu\lambda/3$$

holds for each n_j , which contradicts

$$\lim_{n_j \rightarrow \infty} E\left(|H_{\mathbf{j}^{(m_{n_j})}, b_{n_j}}|^r \mathbb{I}\{|H_{\mathbf{j}^{(m_{n_j})}, b_{n_j}}| > C\}\right) = E(|Y|^r \mathbb{I}\{|Y| > C\}) < \nu\lambda/3,$$

that follows by DCT from $H_{\mathbf{j}^{(m_{n_j})}, b_{n_j}} \xrightarrow{D} Y$ along with $E(|H_{\mathbf{j}^{(m_{n_j})}, b_{n_j}}|^r) \rightarrow E(|Y|^r)$ from the assumed moment conditions.

Now, the remaining is to show $\lim_{n \rightarrow \infty} E \left(H_{\mathbf{j}(n),n}^2 \right) = E(Y^2)$. By 4th-order stationarity we only need to prove $\lim_{n \rightarrow \infty} E(H_n^2) = \sigma^2(\psi)$. By Assumption 1, (Brillinger, 2001), and (Fuentes, 2002) we have,

$$E(I_n(\omega)) = f(\omega) + O(n^{-1}), \quad \omega \in \Pi^2 \quad (16)$$

and for $\omega_1, \omega_2 \in \Pi^2$, and $i = 1, 2$,

$$\text{Cov}(I_n(\omega_1), I_n(\omega_2)) = \begin{cases} f^2(\omega_1) + O(n^{-1}) & \text{if } |\omega_{1i}| = |\omega_{2i}| (\neq 0, \forall i = 1, 2) \\ \frac{(2\pi)^2}{n} f_4(\omega_1, \omega_2, -\omega_2) + O(n^{-1}) & \text{if } |\omega_{1i}| \neq |\omega_{2i}|. \end{cases} \quad (17)$$

The error terms are uniform in ω . Hence, for $i = 1, 2$,

$$\begin{aligned} \text{Var}(H_n(\psi)) &= n^{-1}(4\pi^2)^2 \sum_{\mathbf{j}, \mathbf{k} \in \mathcal{J}_n} \psi(\omega_{\mathbf{j},n}) \psi(\omega_{\mathbf{k},n}) \text{Cov}(I_n(\omega_{\mathbf{j},n}), I_n(\omega_{\mathbf{k},n})) \\ &= n^{-1}(4\pi^2)^2 \left[\sum_{\mathbf{j} \in \mathcal{J}_n} \psi(\omega_{\mathbf{j},n}) (\psi(\omega_{\mathbf{j},n}) + \psi(-\omega_{\mathbf{j},n})) \text{Var}(I_n(\omega_{\mathbf{j},n})) \right. \\ &\quad \left. + \sum_{\substack{\mathbf{j}, \mathbf{k} \in \mathcal{J}_n \\ |\omega_{j_i}| \neq |\omega_{k_i}|}} \psi(\omega_{\mathbf{j},n}) \psi(\omega_{\mathbf{k},n}) \text{Cov}(I_n(\omega_{\mathbf{j},n}), I_n(\omega_{\mathbf{k},n})) \right] \\ &=: S_1 + S_2. \end{aligned}$$

By Eq. (17) and Riemann sum form, it holds that

$$\begin{aligned} S_1 &= (2\pi)^2 n^{-1} 4\pi^2 \sum_{\mathbf{j} \in \mathcal{J}_n} \psi(\omega_{\mathbf{j},n}) (\psi(\omega_{\mathbf{j},n}) + \psi(-\omega_{\mathbf{j},n})) f^2(\omega_{\mathbf{j},n}) + O(n^{-1}) \\ &= (2\pi)^2 \int_{\Pi^2} \psi(\omega) (\psi(\omega) + \psi(-\omega)) f^2(\omega) d\omega + O(n^{-1}) = \sigma_1^2(\psi) + O(n^{-1}). \end{aligned}$$

Similarly, we have that

$$\begin{aligned} S_2 &= n^{-1} (4\pi^2)^2 \sum_{\substack{\mathbf{j}, \mathbf{k} \in \mathcal{J}_n \\ |\omega_{j_i}| \neq |\omega_{k_i}|}} \psi(\omega_{\mathbf{j},n}) \psi(\omega_{\mathbf{k},n}) \left(\frac{(2\pi)^2}{n} f_4(\omega_{\mathbf{j},n}, \omega_{\mathbf{k},n}, -\omega_{\mathbf{k},n}) + O(n^{-1}) \right) \\ &= (2\pi)^2 n^{-2} 4\pi^2 \left[\sum_{\mathbf{j}, \mathbf{k} \in \mathcal{J}_n} \psi(\omega_{\mathbf{j},n}) \psi(\omega_{\mathbf{k},n}) f_4(\omega_{\mathbf{j},n}, \omega_{\mathbf{k},n}, -\omega_{\mathbf{k},n}) \right. \\ &\quad \left. - \sum_{\mathbf{j} \in \mathcal{J}_n} \psi(\omega_{\mathbf{j},n}) (\psi(\omega_{\mathbf{j},n}) + \psi(-\omega_{\mathbf{j},n})) f_4(\omega_{\mathbf{j},n}, \omega_{\mathbf{j},n}, -\omega_{\mathbf{j},n}) + O(n^{-1}) \right] \\ &= (2\pi)^2 \int_{\Pi^2} \int_{\Pi^2} \psi(\omega_1) \psi(\omega_2) f_4(\omega_1, \omega_2, -\omega_2) d\omega_1 d\omega_2 + O(n^{-1}) = \sigma_2^2(\psi) + O(n^{-1}). \end{aligned}$$

Now, we have $\text{Var}(H_n(\psi)) = \sigma_1^2(\psi) + \sigma_2^2(\psi) + O(n^{-1}) = \sigma^2(\psi) + O(n^{-1})$. By Eq. (16) and bounded variation of $\psi(\cdot)$, we also have

$$E(H_n(\psi)) = n^{1/2} \left(\frac{(2\pi)^2}{n} \sum_{\mathbf{j} \in \mathcal{J}_n} \psi(\omega_{\mathbf{j},n}) \{f(\omega_{\mathbf{j},n}) + O(n^{-1})\} - \int_{\Pi^2} \psi(\omega) f(\omega) d\omega \right) = O(n^{-1/2}).$$

Hence, we conclude that $E(H_n(\psi))^2 = \text{Var}(H_n(\psi)) + E^2(H_n(\psi)) = \sigma^2(\psi) + O(n^{-1})$.

Finally, we prove statement (ii), i.e., we will show $\sup_{x \in \mathbb{R}} |\widehat{F}_{n,C}(x) - F_n(x)| \xrightarrow{P} 0$ as $n \rightarrow \infty$. Let Y_n^* denotes a random variable with distribution function \widehat{F}_n , then $(Y_n^* - \widehat{t}_n^{(1)})$ is a random variable with distribution function $\widehat{F}_{n,C}$. Because $\sup_{x \in \mathbb{R}} |\widehat{F}_n(x) - F(x)| \xrightarrow{P} 0$ and $\widehat{t}_n^{(1)} \xrightarrow{P} t_n^{(1)}$, and $t_n^{(1)} \rightarrow E(Y) = 0$ guaranteed by the moment assumption, we have, for any sub-sequence $\{n_j\} \subset \{n\}$, there exists a further sub-sequence $\{n_k\} \subset \{n_j\}$ such that $Y_{n_k}^* \xrightarrow{D} Y$ and $\widehat{t}_{n_k}^{(1)} \rightarrow 0$ hold as $n_k \rightarrow \infty$ almost surely (a.s.). By Slutsky's theorem, $(Y_{n_k}^* - \widehat{t}_{n_k}^{(1)}) \xrightarrow{D} Y$ follows a.s. which, because $\{n_j\}$ was arbitrary, implies $\sup_{x \in \mathbb{R}} |\widehat{F}_{n,C}(x) - F(x)| \xrightarrow{P} 0$. Statement (ii) follows from a triangle inequality. \square

Proof of Lemma A.2

Note that,

$$\begin{aligned} & (2\pi)^2 b^{-1} \sum_{\mathbf{j} \in \mathcal{J}_b} \psi(\omega_{\mathbf{j},b}) \frac{1}{L} \sum_{\ell=1}^L \left(\mathcal{I}_{\text{sub}}^{(\ell)}(\omega_{\mathbf{j},b}) - \widetilde{\mathcal{I}}_n(\omega_{\mathbf{j},b}) \right)^2 \\ &= (2\pi)^2 b^{-1} \left[\sum_{\ell=1}^L \psi(\omega_{\mathbf{j},b}) \left(\frac{1}{L} \sum_{\ell=1}^L (\mathcal{I}_{\text{sub}}^{(\ell)}(\omega_{\mathbf{j},b}))^2 - 2f^2(\omega_{\mathbf{j},b}) \right) \right. \\ & \quad \left. + \sum_{\ell=1}^L \psi(\omega_{\mathbf{j},b}) \left(f^2(\omega_{\mathbf{j},b}) - (\widetilde{\mathcal{I}}_n(\omega_{\mathbf{j},b}))^2 \right) + \sum_{\ell=1}^L \psi(\omega_{\mathbf{j},b}) f^2(\omega_{\mathbf{j},b}) \right] \\ &=: S_{1n} + S_{2n} + S_{3n}. \end{aligned}$$

It is immediate from the Riemann sum expression that, $S_{3n} \rightarrow \int_{\Pi^2} \psi(\omega) f^2(\omega)$ as $n \rightarrow \infty$. Now, proceeding in the same way as (Yu, 2023), using Cauchy-Schwarz inequality and boundedness of $\psi(\cdot)$ we have $|S_{2n}| = o(1)$. Also, using the moment conditions we have $S_{1n} \xrightarrow{P} 0$, which gives us the statement of Lemma A.2. \square

Supplementary Material

Supplementary Material for Frequency Domain Resampling for Gridded Spatial Data.

In this supplementary material we present more simulation results for finite samples in support of the proposed method.

References

- BANDYOPADHYAY, S., JENTSCH, C. and RAO, S. S. (2017). A spectral domain test for stationarity of spatio-temporal data. *Journal of Time Series Analysis* **38** 326–351.
- BANDYOPADHYAY, S. and LAHIRI, S. N. (2010). Asymptotic properties of Discrete Fourier transforms for spatial data. *Sankhya* **71** 221–259.
- BANDYOPADHYAY, S., LAHIRI, S. N. and NORDMAN, D. J. (2015). A frequency domain empirical likelihood method for irregularly spaced spatial data. *The Annals of Statistics* **43** 519–545.
- BANDYOPADHYAY, S. and RAO, S. S. (2016). A test for stationarity for irregularly spaced spatial data. *Journal of the Royal Statistical Society: Series B* **79** 95–123.
- BERAN, J. (1992). A goodness-of-fit test for time series with long range dependence. *Journal of the Royal Statistical Society Series B: Statistical Methodology* **54** 749–760.
- BRILLINGER, D. R. (2001). *Time Series*. Society for Industrial and Applied Mathematics, Philadelphia, PA.
- CRESSIE, N. A. C. (1993). *Statistics for Spatial Data*, revised ed. Wiley.
- CRUJEIRAS, R. M. and FERNANDEZ-CASAL, R. (2010). On the estimation of the spectral density for continuous spatial processes. *Statistics* **44** 587–600.
- DAHLHAUS, R. (1985). Asymptotic normality of spectral estimates. *Journal of Multivariate Analysis* **16** 412–431.
- DAHLHAUS, R. and JANAS, D. (1996). A frequency domain bootstrap for ratio statistics in time series analysis. *The Annals of Statistics* **24** 1934–1963.
- DAVISON, A. C. and HINKLEY, D. V. (1997). *Bootstrap methods and their application* **1**. Cambridge university press.
- FUENTES, M. (2002). Spectral methods for nonstationary spatial processes. *Biometrika* **89** 197–210.
- FUENTES, M. (2006). Testing for separability of spatial-temporal covariance functions. *Journal of Statistical Planning and Inference* **136** 447–466.
- FUENTES, M. (2007). Approximate likelihood for large irregularly spaced spatial data. *Journal of the American Statistical Association* **102** 321–331.
- GUAN, Y., SHERMAN, M. and CALVIN, J. A. (2004). A nonparametric test for spatial isotropy using subsampling. *Journal of the American Statistical Association* **99** 810–821.
- HALL, P., FISHER, N. I. and HOFFMAN, B. (1994). On the nonparametric estimation of covariance functions. *Annals of Statistics* **22** 2115–2134.
- IM, H. K., STEIN, M. L. and ZHU, Z. (2007). Semiparametric estimation of spectral density with irregular observations. *Journal of the American Statistical Association* **102** 726–735.
- JENTSCH, C. and KREISS, J.-P. (2010). The multiple hybrid bootstrap—resampling multivariate linear processes. *Journal of Multivariate Analysis* **101** 2320–2345.
- KREISS, J.-P. and LAHIRI, S. N. (2012). Bootstrap methods for time series. In *Handbook of statistics*, **30** 3–26. Elsevier.
- KREISS, J.-P. and PAPARODITIS, E. (2003). Autoregressive-aided periodogram bootstrap for timeseries. *The Annals of Statistics* **31** 1923–1955.
- KREISS, J.-P., PAPARODITIS, E. and POLITIS, D. N. (2011). On the range of validity of the autoregressive sieve bootstrap. *Annals of Statistics* 2103–2130.
- KREISS, J.-P. and PAPARODITIS, E. (2012). The hybrid wild bootstrap for time series. *Journal of the American Statistical Association* **107** 1073–1084.
- KREISS, J.-P. and PAPARODITIS, E. (2023). Bootstrapping Whittle estimators. *Biometrika* **110** 499–518.
- LAHIRI, S. N. (2003). *Resampling methods for dependent data*. Springer Science & Business Media.
- LI, W. and MCLEOD, A. (1986). Fractional time series differencing. *Biometrika* **73** 217–221.
- LJUNG, G. M. and BOX, G. E. (1978). On a measure of lack of fit in time series models. *Biometrika* **65** 297–303.
- MATSUDA, Y. and YAJIMA, Y. (2009). Fourier analysis of irregularly spaced data on Rd. *Journal of the Royal Statistical Society: Series B* **71** 191–217.
- MEYER, M., PAPARODITIS, E. and KREISS, J.-P. (2020). Extending the validity of frequency domain bootstrap methods to general stationary processes. *The Annals of Statistics* **48** 2404–2427.
- MILHØJ, A. (1981). A test of fit in time series models. *Biometrika* **68** 177–187.
- NG, W. L., YAU, C. Y. and CHEN, X. (2021). Frequency domain bootstrap methods for random fields. *Electronic Journal of Statistics* **15** 6586–6632.

- NORDMAN, D. J. and LAHIRI, S. N. (2004). On optimal spatial subsample size for variance estimation. *The Annals of Statistics* **32** 1981–2027.
- NORDMAN, D. J. and LAHIRI, S. N. (2006). A frequency domain empirical likelihood for short-and long-range dependence. *The Annals of Statistics* 3019–3050.
- PAPARODITIS, E. (2000). Spectral density based goodness-of-fit tests for time series models. *Scandinavian Journal of Statistics* **27** 143–176.
- PARZEN, E. (1957). On consistent estimates of the spectrum of a stationary time series. *The Annals of Mathematical Statistics* 329–348.
- POLITIS, D. N. and MCELROY, T. S. (2019). *Time series: A first course with bootstrap starter*. CRC Press.
- POLITIS, D. N., ROMANO, J. P. and WOLF, M. (1999). *Subsampling*. Springer Science & Business Media.
- SHERMAN, M. (1996). Variance estimation for statistics computed from spatial lattice data. *Journal of the Royal Statistical Society Series B: Statistical Methodology* **58** 509–523.
- SHERMAN, M. (1998). Efficiency and robustness in subsampling for dependent data. *Journal of statistical planning and inference* **75** 133–146.
- SHERMAN, M. and CARLSTEIN, E. (1994). Nonparametric estimation of the moments of a general statistic computed from spatial data. *Journal of the American Statistical Association* **89** 496–500.
- STEIN, M. L. (1999). *Interpolation of spatial data: some theory for kriging*. Springer Science & Business Media.
- SUBBA RAO, S. (2018). Statistical inference for spatial statistics defined in the Fourier domain. *The Annals of Statistics* **46** 469–499.
- TANIGUCHI, M. (1979). On estimation of parameters of Gaussian stationary processes. *Journal of Applied Probability* **16** 575–591.
- VAN HALA, M., BANDYOPADHYAY, S., LAHIRI, S. N. and NORDMAN, D. J. (2017). On the non-standard distribution of empirical likelihood estimators with spatial data. *Journal of Statistical Planning and Inference* **187** 109–114.
- VAN HALA, M., BANDYOPADHYAY, S., LAHIRI, S. N. and NORDMAN, D. J. (2020). A general frequency domain method for assessing spatial covariance structures. *Bernoulli* **26** 2463–2487.
- WELLER, Z. D. and HOETING, J. A. (2020). A nonparametric spectral domain test of spatial isotropy. *Journal of statistical planning and inference* **204** 177–186.
- YU, H. (2023). Resampling-based inference for time series in the frequency domain, PhD thesis, Iowa State University PhD Thesis.
- YU, H., KAISER, M. S. and NORDMAN, D. J. (2023). A subsampling perspective for extending the validity of state-of-the-art bootstraps in the frequency domain. *Biometrika* asad006.

Supplementary Material for Frequency Domain Resampling for Gridded Spatial Data

SOUVICK BERA^{1,a}, DANIEL J. NORDMAN^{2,c} and SOUTIR BANDYOPADHYAY^{1,b}

¹Department of Applied Mathematics and Statistics, Colorado School of Mines, Golden, CO 80401, USA,

^aberasouvik@mines.edu, ^bsbandyopadhyay@mines.edu

²Department of Statistics, Iowa State University, Ames, IA 50011, USA, ^cdnordman@iastate.edu

Keywords: Spatial Frequency Domain Bootstrap; Periodogram; Spectral Mean

1. Numerical Studies of Accuracy

For a comprehensive comparison and to complete the simulation study presented in Section 5, we further investigate the performance of the FDWB and HFDB methods for inferring spectral means for non-Gaussian spatial processes, particularly focusing on scenarios where $\sigma_2^2 \approx 0$. This comparison aims to highlight the effectiveness of both approaches in cases where σ_2^2 is very close to zero. By examining these scenarios, our overall goal is to demonstrate the robustness and accuracy of the HFDB method in a wider range of conditions. Moreover, we seek to confirm that the HFDB-based estimator performs adequately in situations where σ_2^2 is low, as expected theoretically. This detailed analysis further ensures that our findings are thorough and applicable to various practical situations involving non-Gaussian spatial processes.

1.1. Results for Non-Gaussian Process

For non-Gaussian processes with low σ_2^2 values, we considered the Gaussian-Log-Gaussian process as described in ?. We generated datasets of sizes 30×30 ($n = 900$), 50×50 ($n = 2500$), and 70×70 ($n = 4900$) on regularly spaced square-shaped lattice regions. For each dataset size, we ran 500 Monte Carlo simulations for coverage and 500 simulations to generate the bootstrap distributions. This process was examined for different range parameters with the scalar parameter as 0.01 (see ? for more details on the rationale behind this choice where the scalar parameter is denoted by ν). This setup allows us to evaluate the performance of our proposed methods in a context where σ_2^2 is small but not zero, providing insight into their effectiveness under these specific conditions.

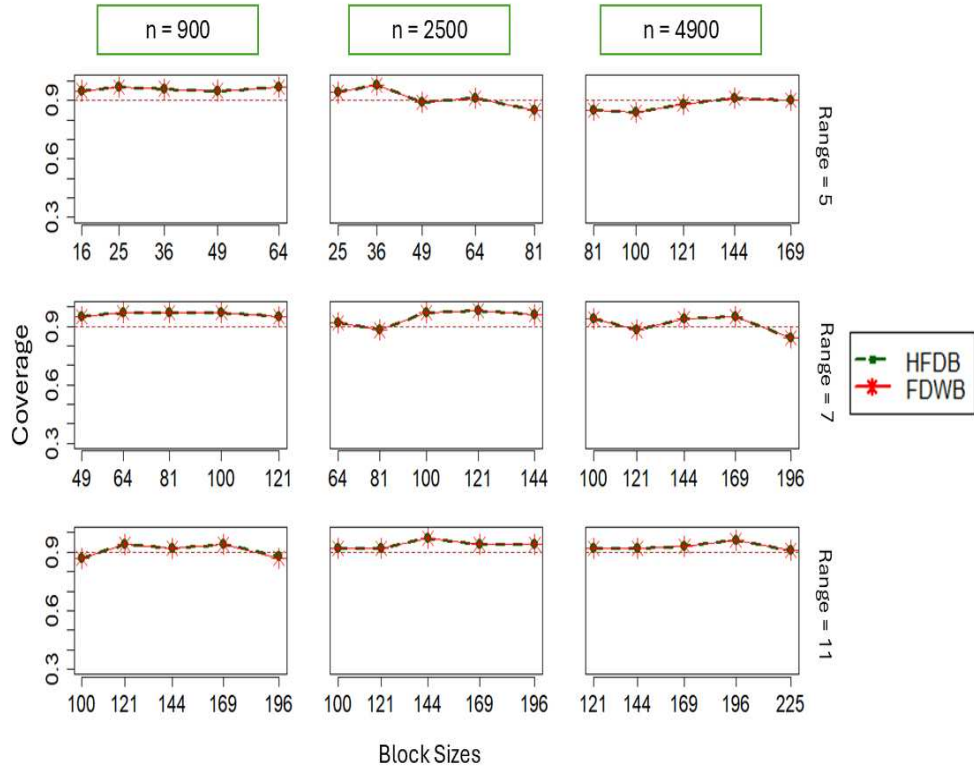


Figure 1. Coverages of 90% HFDB intervals for the covariance parameter $\gamma(\mathbf{h}), \mathbf{h} = (1, 0)^T$, based on either non-corrected ($Q_{FDWB,n}^*(\psi)$) (red line) or corrected ($H_{HFDB,n}^*(\psi)$) (green line) HFDB versions with different subsample sizes b_n , range, and sample sizes n .

We note from Figure 1 that both methods perform similarly when σ_2^2 is very small. This contrasts with the results in Figure 2 of Section 5, where there is a significant difference in the performance of the two methods due to a higher value of σ_2^2 . We further observe that as the subsample size b_n and the overall sample size n increase, the coverage accuracy improves across different range parameters.

2. Application to Calibrating Spatial Isotropy Tests

As described in Section 6, the simulation results for a sample region 30×30 , using the same parameters as before for both Gaussian and non-Gaussian processes, are based on 1000 simulations at a 10% nominal level and are as follows.

Table 1. Rejection rates for Gaussian data.

τ_R	Subsampling	FDWB	HFDB
1	0.071	0.108	0.108
1.1	0.107	0.14	0.14
1.2	0.236	0.324	0.324
1.3	0.563	0.646	0.646
1.4	0.845	0.92	0.92
1.5	0.914	0.966	0.966
1.6	0.992	1	1

Table 2. Rejection rates for Non-Gaussian data.^a

τ_R	Subsampling	HFDB
1	0.066	0.105
1.2	0.101	0.127
1.4	0.325	0.464
1.6	0.62	0.743
1.8	0.873	0.922
2	0.987	1

^aFor non-Gaussian data, FDWB fails to maintain the size at the 10% level, with a rejection rate of 0.277 for $\tau_R = 1$, indicating its inappropriateness for such data.

The tables indicate that all frequency domain resampling methods perform well when the underlying distribution is Gaussian, as expected. However, under non-Gaussianity, FDWB fails to maintain size under isotropy, making it unsuitable for such scenarios. In contrast, both HFDB and subsampling remain effective even with smaller sample sizes.